

ISTANBUL TECHNICAL UNIVERSITY ★ ENERGY INSTITUTE

**OPTIMUM DESIGN OF HELIX GROUND HEAT EXCHANGERS
FOR HEAT PUMP APPLICATIONS**



M.Sc. THESIS

Babak DEGHAN

Energy Science and Technology Division

Energy Science and Technology Program

May 2015

ISTANBUL TECHNICAL UNIVERSITY ★ ENERGY INSTITUTE

**OPTIMUM DESIGN OF HELIX GROUND HEAT EXCHANGERS
FOR HEAT PUMP APPLICATIONS**



M.Sc. THESIS

**Babak DEGHAN
(301131004)**

Energy Science and Technology Division

Energy Science and Technology Program

Thesis Advisor: Prof. Dr. Altug SISMAN

May 2015

İSTANBUL TEKNİK ÜNİVERSİTESİ ★ ENERJİ ENSTİTÜSÜ

**ISI POMPASI UYGULAMALARI İÇİN HELİS TİPİ TOPRAK ISI
DEĞİŞTİRİCİLERİNİN OPTIMUM TASARIMI**

YÜKSEK LİSANS TEZİ

**Babak DEHGHAN
(301131004)**

Enerji Bilim ve Teknoloji Anabilim Dalı

Enerji Bilim ve Teknoloji Programı

Tez Danışmanı: Prof. Dr. Altuğ ŞİŞMAN

Mayıs 2015



FOREWORD

My sincere gratitude and thanks to my supervisor, Prof. Dr. Altug SISMAN, for his phenomenal kindness, expertise guidance and continuous support throughout my research in Istanbul Technical University Energy Institute.

I would like to thank the members of my thesis examination committee, for spending their precious time on reading my thesis and sharing their expertise.

Special gratitude goes to my working partner Mr Murat AYDIN for his help during the project implementation.

Finally, I am deeply thankful to my parents for their endless love, unconditional support and fortitude in the pursuit of my academic goals.

May 2015

Babak DEGHAN
(Member of New Energy
Technologies Research Group)



TABLE OF CONTENTS

FOREWORD	vii
TABLE OF CONTENTS	ix
ABBREVIATIONS	xi
LIST OF TABLES	xiii
LIST OF FIGURES	xiii
Nomenclature	xv
SUMMARY	xvii
ÖZET	xix
1. INTRODUCTION	1
1.1 Purpose of Thesis	3
1.2 Literature Review	3
1.3 Present Study	8
2. GROUND SOURCE HEAT PUMP	11
2.1 Heat Pump	11
2.1.1 Overview	12
2.1.2 The reversed Carnot cycle.....	12
2.1.3 The ideal vapor compression refrigeration cycle	14
2.1.4 Actual vapor compression refrigeration cycle	16
2.1.5 Heat sources	18
2.1.5.1 Air	19
2.1.5.2 Soil	19
2.1.5.3 Water	19
2.2 Ground Source Heat Pump Systems	20
2.2.1 Ground heat exchanger	21
2.2.1.1 History.....	22
2.2.1.2 Need of ground heat exchanger.....	22
2.2.1.3 Mechanism of heat transfer.....	23
2.2.2 Open Loop systems	24
2.2.3 Closed Loop systems	25
2.2.3.1 Horizontal closed loops.....	25
2.2.3.2 Pond and lake loops	26
2.2.3.3 Vertical closed loops	27
2.2.4 The benefits of GSHPs.....	28
3. EXPERIMENTAL SETUPS	31
3.1 Ground Source Heat Pump Test and Research Laboratory.....	31
3.1.1 GHE test system.....	33
3.1.2 Heat pump test system and and example for COP measurement	35
3.2 Shallow GHE Test Results	37
3.3 Helix GHE Test Conditions and Results.....	37
4. SIMULATION	41
4.1 Modeling Purpose	41
4.2 Model Description.....	41

4.3 Single Helix GHEs Computational Results and Validations	43
4.4 Computational Results for Multi Vertical Helix GHE and Examination of Performance Loss	45
4.4.1 Prediction of performance losses	45
4.4.2 Determination of temperature distribution around GHEs	48
4.5 The Influences of the Pitch Distance (L_p) and Major Diameter (D) of a Single Vertical Helix GHE on it's HTR Value.....	52
4.6 A Typical Example for Vertical Helix GHE Analysis	55
5. CONCLUSIONS AND RECOMMENDATIONS	59
REFERENCES	61
APPENDIX A :	65
CURRICULUM VITAE.....	67



ABBREVIATIONS

CFD	: Computational Fluid Dynamic
cGHE	: Critical Ground Heat Exchanger
COP	: coefficient of performance
GHE	: Ground Heat Exchanger
GSHP	: Ground Source Heat Pump
HTR	: Heat Transfer Rate
ITU	: Istanbul Technical University
sGHE	: Single Ground Heat Exchanger
TRT	: Thermal Response Test



LIST OF TABLES

	<u>Page</u>
Table 3.1: Properties of different boreholes at Energy Institute of ITU	31
Table 3.2: Different types of GHE at ITU Energy Institute	33
Table 3.3: Heat pump COP test results.	36
Table 3.4: Characteristics of the helical-shape GHE pipes	38
Table 3.5: Characteristics of ground and working conditions	38



LIST OF FIGURES

	<u>Page</u>
Figure 1.1 : Cause and effect diagram for GSHP system (Sivasakthivel et al, 2014).	3
Figure 1.2 : Helical horizontal ground heat exchanger configuration considered in the simulations (Congedo et al, 2012).....	4
Figure 1.3 : Temperature profiles along the three helix GHE with different Fourier number (Fo) obtained by Cui et al (2011).....	5
Figure 1.4 : Vertical GHE and configurations (Sagia et al, 2012).....	7
Figure 1.5 : Cross-section of a vertical GHE. The fluid is ascending in one pipe and descending in the other,(Koohi-Fayegh and Rosen, 2012).	7
Figure 2.1 : Simplified model of a heat pump system.	12
Figure 2.2 : P-v and T-s diagrams of a reversed Carnot cycle.	13
Figure 2.3 : Schematic and T-s diagram for the ideal vapor compression refrigeration cycle (URL-2)	15
Figure 2.4 : P-h diagram of ideal vapor compression refrigeration cycle.....	16
Figure 2.5 : T-s diagram of the actual vapor compression refrigeration cycle.	17
Figure 2.6 : Real process of a vapor compression heat pump cycle.	18
Figure 2.7 : GSHP Schematic view.	21
Figure 2.8 : Open-loop system (Banks, 2008)	25
Figure 2.9 : Horizontal closed loops GHEs (URL-2)	26
Figure 2.10 : Heat transfer mechanisms in shallow ponds (Banks, 2008).....	26
Figure 2.11 : Schematic view of U-tube and helical GHEs (URL2)	27
Figure 2.12 : Closed-loop systems (Banks, 2008)	28
Figure 3.1 : Different boreholes in laboratory	31
Figure 3.2 : Vertical helix GHE.....	32
Figure 3.3 : Spiral and slinky GHE.....	33
Figure 3.4 : Experimental Test System.....	34
Figure 3.5 : Constant Temperature TRT System	34
Figure 3.6 : Connection interface of heat pump COP test system	35
Figure 3.7 : COP cooling and heating test results.....	36
Figure 3.8 : Shallow GHE test results (Aydin et all, 2015).	37
Figure 3.9 : Inlet and outlet water temperature evaluation in 120 hours operation. .	39
Figure 3.10 : HTR of helix GHE for 120 hours non-stop operation.....	40
Figure 3.11 : Ground temperature variation at ITU Energy Institute field.	40
Figure 4.1 : Different configurations of vertical helix GHEs	41
Figure 4.2 : Horizontal helix GHE COMSOL model	42
Figure 4.3 : Schematic view of helix GHE.	42
Figure 4.4 : Single horizontal and vertical helix GHE model validation for 120 hours non-stop operation experiment.....	44
Figure 4.5 : Numerical temperature distribution in the ground at the end of 3months operation around single veryical helix GHE	45
Figure 4.6 : Temperature distribution around single helix GHE at the end of one, two and three months.	45

Figure 4.7 : Performance losses of critical GHE at the end of 3months non-stop operation.....	47
Figure 4.8 : Schematic diagram of a GSHP system with three helix GHEs (Cui et al, 2011).....	47
Figure 4.9 : Time dependency of performance losses in case of 7 meter distance between GHEs	48
Figure 4.10 : Effect of distance between GHEs in temperature distribution at $z=1.5\text{m}$ and at the end of 3months non-stop operation for (a) $N=2$ (b) $N=3$ (c) $N=5$	50
Figure 4.11 : Temperature distribution in the ground at the end of 1, 2, 3 months non-stop operation for (a) $N=2$ (b) $N=3$ (c) $N=5$	51
Figure 4.12 : Schematic top view of temperature distribution in the ground at the end of 3 month non-stop operation with $d=7\text{ m}$	52
Figure 4.13 : Effect of pitch (L_p) on HTR for 3 months non-stop operation	53
Figure 4.14 : Effect of GHE major radius (D) on HTR for three months non-stop operation	54
Figure 4.15 : HTR value of a single helix GHE versus L_p for different operation times	54
Figure 4.16 : HTR of a single helix GHE versus D for different operation times	55
Figure 4.17 : Building with vertical helix GHE.....	56
Figure 4.18 : Nine vertical helix configuration.....	57
Figure 4.19 : Thermal interaction between nine vertical helix GHEs for 6 month non-stop operation	57
Figure 4.20 : Other configuration type of nine vertical helix GHEs.....	58
Figure A.1: ITU Energy Institute laboratory schematic view.....	66

Nomenclature

C_p	: Specific heat capacity of ground [$\text{J Kg}^{-1} \text{K}^{-1}$]
C_{PE}	: Specific heat capacity of polyethylene tube [$\text{J Kg}^{-1} \text{K}^{-1}$]
D	: GHE diameter [mm]
d	: Distance between borehole [mm]
Fo	: Fourier number
k_{PE}	: Thermal conductivity of polyethylene tube [$\text{W m}^{-1} \text{K}^{-1}$]
k_{eff}	: Effective thermal conductivity [$\text{W m}^{-1} \text{K}^{-1}$]
L_p	: Pitch between helix turns [mm]
L_{GHE}	: GHE vertical length [mm]
n	: Number of turns
N	: Number of GHE
$\overline{\dot{Q}}_{sGHE}$: Time average value of HTR of a single GHE [W]
$\overline{\dot{Q}}_{cGHE}$: Time average value of HTR of the critical GHE [W]
r_i	: Internal radius of polyethylene tube [mm]
r_o	: External radius of polyethylene tube [mm]
r_H	: radial coordinates of helix GHE surface [mm]
T_{avg-i}	: Average temperature of inlet water [$^{\circ}\text{C}$]
T_{avg}	: Average water condition [$^{\circ}\text{C}$]
T_e	: Undisturbed mean ground temperature [$^{\circ}\text{C}$]
T_{avg-o}	: Average temperature of outlet water [$^{\circ}\text{C}$]
Z	: Depth from the surface [mm]
z_H	: Axial coordinates of helix GHE surface [mm]
α	: Thermal diffusivity of ground
ρ_{PE}	: Density of polyethylene tube [Kg m^{-3}]
ρ	: Density of ground [Kg m^{-3}]



OPTIMUM DESIGN OF HELIX GROUND HEAT EXCHANGERS FOR HEAT PUMP APPLICATIONS

SUMMARY

Efficient use of energy allows decreasing energy consumption as well as less environmental pollution and leads to sustainable development. For an efficient way of heating and cooling of spaces, ground can be used as an energy storage medium for heat exchange processes of heat pump systems to reach higher efficiency. These types of systems are called ground source heat pump (GSHP) systems, which are well established in Western and European countries for space heating and cooling applications. The installation cost and performance of GSHP systems can be greatly affected by optimal design of ground heat exchangers (GHEs).

One of the most important GHEs that is used these days is helix GHEs. These GHEs are cheaper than others and also have some advantages. Three parameters affecting the helix GHE's performance are GHEs spacing, GHE major diameter and helical configuration of the pipe. In large scale GSHP applications, more than one GHE is needed, therefore determining the distance between GHEs becomes as an important issue. In this thesis, the effects of distance between vertical helix GHEs on the heat transfer ratio (HTR) are studied. Performance of GHE is determined and optimal distance is examined. Furthermore, the influence of the pitch between the turns of the helix on HTR and GHE major radius are numerically studied in COMSOL environment. The available experimental data are used to validate the numerical results. It is seen that they are in a good agreement. Computational model in this study may provide useful guidance for designing the helical shaped GHE for GSHP systems.

The heat transfer from/to the pipe wall of the heat exchanger to/from the ground depends on the turns number, location, material and configuration of the pipes. In this study, computer modeling of 1, 2, 3 and 5 helix GHEs are described. For modeling the heat transfer of a GHE, the ground soil/rock is usually approximated as an infinite homogeneous medium and heat transfer is assumed mainly to take place by conduction. The wall temperature of GHE is assumed as constant and average value of inlet and outlet water temperature. Performance losses due to thermal interactions for different GHE spacings are determined for different number of helix GHEs. Distances between GHEs vary from 1 m to 11 m. Also different characteristics of soil in the ground and its temperature play an important role in GHE performance. The temperature of the ground around GHE is a function of the soil thermal properties like thermal diffusivity (α), thermal conductivity (k) and the heat capacity (C_p) as well as temperature of fluid, time, position. The soil thermal diffusivity is a defined property and is the ratio of the thermal conductivity and the volumetric heat capacity. Therefore, three soil properties (k , α and C_p) should be known or estimated to predict the thermal behavior of GHEs. Obtaining accurate

values of the thermal properties of the soil requires a detailed site survey. Soil composition varies widely not only with locations but also from wet clay to sandy soil.

In order to better understand the behavior of the system, the performance of the GHE is experimentally analyzed for 5 day non-stop operation. Evolution of inlet and outlet temperatures for vertical helix circuits are measured. It is seen that inlet temperature is almost constant as 40 °C. The outlet temperature reaches the maximum value of 39.2 °C. It is also observed that the outlet temperature gets higher values for longer operation times, due to increment of soil temperature. Based on the observation of temperature change, we consider that the temperature of the pipe's wall is almost constant and is equal to the average value of inlet and outlet temperature amounts.

Furthermore, a single helix GHE 3D model is made using COMSOL multi-physics program based on the geometrical parameter and thermal properties of solid domains (ground, grout, and polyethylene inlet and outlet pipes). The model conditions is the same as the experimental conditions. The accuracy of the model is proved by experimental data. After validating single helix GHE with experimental results, the same model is extended for 2, 3 and 5 GHEs in order to determine their HTR values and performance losses due to their thermal interactions.

Based on the single GHE results, the same study is repeated for 2, 3 and 5 GHEs. The amount of HTR in critical GHE is determined computationally and performance losses are calculated. Critical GHE is defined as central GHE in all part of this thesis. As a result of the study, when the number of GHEs is increased in a finite size domain, increment of the system performance becomes smaller for addition of each GHE. It is found that when the distance between GHEs is $d=3\text{m}$, performance losses of critical GHE (cGHE) for the cases of 2, 3 and 5 GHEs are around 6%, 14% and 22% respectively. Similarly when the distance is 10 m, performance loss is 1%, 2% and 4% for 2, 3 and 5 number of GHEs.

Furthermore, the effects of pitch distance (L_p) and major radius (D) on performance of GHE are investigated. The results of the simulations prove that L_p and D important parameters for the design of a GSHP. Although increment of these parameters also improve the performance of GSHP, a higher investment is needed for installation stage. Therefore an optimum size should be found, which minimizes the total cost over the system lifetime.

ISI POMPASI UYGULAMALARI İÇİN HELİS TİPİ TOPRAK ISI DEĞİŞTİRİCİLERİNİN OPTIMUM TASARIMI

ÖZET

Binalardaki enerji tüketimi, gelişmiş ülkelerde tüketilen toplam enerjinin büyük bir kısmını oluşturur. Toprak kaynaklı ısı pompası sistemleri, hem ısıtma hem de soğutmadaki yüksek enerji verimlilikleri nedeniyle yaygınlaşmaktadır. Toprak kaynaklı ısı pompası sistemlerin kurulum bedelleri ve performansları, toprak ısı değiştiricilerinin optimum seviyedeki tasarımından büyük ölçüde etkilenir.

Günümüzde toprak kaynaklı ısı pompası uygulamalarında düşey U borulu toprak ısı değiştiricilerin yanında yatay olarak da uygulanabilen düz, slinky ve helis tipleri de mevcuttur. Bunların en önemlilerinden biri de helis (sarmal) toprak ısı değiştiricilerdir. Bu ısı değiştiriciler diğerlerinden daha ucuz olmakla beraber, daha az yer kaplaması, uygulama kolallığı olması vb. avantajlara da sahiptirler. Sarmal şekillendirmiş toprak ısı değiştiricisinin performansını etkileyen üç etken vardır; Toprak ısı değiştiricisi borular arasındaki aralık, toprak ısı değiştiricisi nominal çapı ve borunun sarmal yapısıdır. Büyük ölçekli toprak kaynaklı ısı pompaları uygulamalarında birden çok toprak ısı değiştiricisi gereklidir, bu yüzden ısı değiştiricilerin arasındaki uzaklığı belirlemek önemli bir konudur. Bu tezde de, sarmal toprak ısı değiştiricilerin aralarındaki mesafenin ısı transfer oranına (ITO) etkileri araştırılmıştır. Toprak ısı değiştiricisi performansı belirlenmiş ve optimum uzaklık tespit edilmiştir. Buna ek olarak, saha ve sarmalların sarımları arasındaki etkinin ısı transfer oranına ve toprak ısı değiştiricisi nominal çapına olan bağı sayısal olarak COMSOL'da araştırmıştır. Elde edilen deneysel veriler de bu sayısal sonuçları doğrulamakta kullanılmıştır ve uyumlu oldukları görülmüştür. Bu çalışmada yapılan sayısal model Toprak kaynaklı ısı pompaları sistemlerindeki sarmal toprak ısı değiştiricileri tasarlamak için bir yararlı bir yol gösterici olacaktır.

Deneysel çalışmalarda kullanılan Helis toprak ısı değiştiricisi Toprak Kaynaklı Isı Pompası Test ve Araştırma Laboratuvarının açık hava bölümünde toprak içerisine yerleştirilmiştir. Toprağa gömülmeden önce yaklaşık 1.1m uzunluğunda olan helis toprak ısı değiştiricisi açılarak ve sabit durmasını sağlayacak bir boru vasıtasıyla 3m uzunluğa getirilmiştir. Daha sonra hazırlanan Helis toprak ısı değiştiricisi açılan kuyunun içerisine alt tabanı yerden 4.5m derinlikte üst kısmı yerden 1.5m derinlikte olacak şekilde yerleştirilmiş ve boşluklar çıkan toprak ile doldurulmuştur. Uçları dışarıda kalan toprak ısı değiştiricisinin uç boruları 0.5m derinlikte toprak altında yalıtımlı borularla laboratuvar içerisinde bulunan Isıl Test Sistemine bağlanmıştır. Gerekli sızdırmazlık testleri yapılarak toprak ısı değiştiricisi incelemelere hazır hale getirilmiş ve test edilmiştir. Farklı zamanlarda birden fazla testler yapılarak sonuçlar doğrulanmıştır.

Sistem durumunun daha iyi anlaşılabilmesi için, toprak ısı değiştiricisinin performansı 5 gün boyunca izlenmiştir. İç ve dış devrelerdeki giriş ve çıkış

sıcaklıklarının değişimi ölçülmüştür. Giriş su sıcaklığı 40 °C'de sabit olarak tutulmuştur. Toprak ısı değiştiricisine giden suyun ortalama dönüş sıcaklığı ise 39.2 °C'dir. Ayrıca toprak sıcaklığındaki artış sebebiyle, topraktan çıkış su sıcaklığının zaman boyunca daha yüksek değerlere ulaştığı gözlenmiştir. Bu sıcaklık davranışına göre, boru duvarlarındaki sıcaklığın sabit olduğu ve giriş ve çıkış sıcaklığının ortalamasına eşit olduğu söylenebilir.

Isı değiştiricinin boru duvarından toprağa olan ısı transferi; sarmal sayısı, konum, malzeme ve boruların yapısına bağlıdır. Toprak ısı değiştiricisinin dışındaki boruları dolduran ana akışkanda, hem taşınım hem de iletimle ısı transferi gerçekleşebilir. Bunun taşınım kısmını ölçmek oldukça zordur. Bu çalışmada 1, 2, 3 ve 5 sarmal şekillendirilmiş toprak ısı değiştiricisinin bilgisayar modellemesi açıklanmıştır. Bir toprak ısı değiştiricisindeki ısı transferini modellemek için, zemindeki toprak/kaya genellikle sonsuz homojen ortam olarak tahmin edilmiş ve ısı transferi çoğunlukla iletimle gerçekleşiyor kabul edilmiştir. Toprak ısı değiştiricisinin duvar sıcaklığı sabit ve giriş ve çıkış su sıcaklıklarının ortalama değeri olarak kabul edilmiştir. Farklı toprak ısı değiştiricisi aralıklarında ısı etkileşimlerinden oluşan performans kayıpları için 3 durum belirlenmiştir. Toprak ısı değiştiricileri arasındaki uzaklık 1 metre ve 11 metre arasında değiştirilmiştir. Ayrıca zemindeki toprağın farklı özellikleri ve sıcaklığı da toprak ısı değiştiricisinin performansında önemli bir rol oynar. Zeminin sıcaklığı toprağın ısıl özelliklerinin bir fonksiyonudur: ısıl yayılım (α), ısıl iletkenlik (k) ve ısı kapasitesi C_p . Toprağın ısıl yayılımı; ısıl iletkenlik ve ısı kapasitesine bağlıdır ve tanımlanmış bir özelliktir. Bu sebeple, toprak ısı değiştiricilerinin ısıl davranışlarını tahmin edebilmek için 3 toprak özelliği: k , α ve C_p , bilinmeli veya hesaplanmalıdır. Toprağın ısıl özelliklerinin doğru değerlerini elde etmek için uygulama yapılacak bölgede ölçüm şarttır. Bu ölçüm işlemi toprağa ısı vererek toprağın buna tepkisinin izlendiği ısıl tepki testleri ile gerçekleştirilir. Toprak bileşimi yalnızca konuma bağlı olarak değil aynı zamanda toprağın yapısına göre de değişim gösterebilir. Toprağın nemlilik oranı, kil, kaya, kum vb. yapısı performansa etki eden faktörlerdendir.

3 boyutlu, tek sarmal toprak ısı değiştirici modeli COMSOL Multifizik programı kullanılarak, geometrik değişkenlere ve katı alanların (zemin, harç ve polietilen giriş ve çıkış boruları) özelliklerine bağlı olarak oluşturulmuştur. Model koşulları deneysel koşullarla aynıdır. Modelin doğruluğu deneysel verilerle kanıtlanmıştır. Tek sarmal toprak ısı değiştiricisi deneysel sonuçları modelledikten sonra, performanslarının belirlenmesi amacıyla bir, iki, üç ve beş sarmal toprak ısı değiştiricisi için modeller oluşturulmuştur. Kritik toprak ısı değiştiricisindeki ısı transferi miktarı sayısal olarak belirlenmiş ve tek sarmal toprak ısı değiştiricisi perasyonunda oluşan performans kayıpları hesaplanmıştır. Kritik toprak ısı değiştiricisi, tüm tez bölümlerinde merkezi toprak ısı değiştiricisi olarak tanımlanmıştır. Bu çalışmanın sonucu olarak, toprak ısı değiştiricilerinin sarmal sayısı arttığında, bütün sistemin verimliliğinin, özellikle toprak ısı değiştiriciler arası mesafe kısa olduğunda, azaldığı görülmüştür. Örneğin, 2 toprak ısı değiştiricisinde merkezi toprak ısı değiştiricisinin performans kaybı, yarıçap 3 m olduğunda % 6'dır. Bu kayıp 3 sarmal toprak ısı değiştiricisinde % 14, 5 sarmal toprak ısı değiştiricisinde % 22'dir. Benzer şekilde, mesafe 10 metre olduğunda performans kaybı 2, 3 ve 5 sarmal toprak ısı değiştiricisi için sırasıyla % 1, % 2 ve % 3'tür.

Buna ek olarak, saha mesafesinin (L_p) ve toprak ısı değiştiricisinin çapının (D) etkisi incelenmiştir. Simülasyonun sonuçları saha mesafesinin ve ısı değiştiricisi çapının toprak kaynaklı ısı pompası sistemlerinin tasarlanmasında önemli parametreler

olduđunu kanıtlamaktadır. Bu deęişkenleri artırmak toprak kaynaklı ısı pompasının verimini artırırsa da, aynı zamanda ilk yatırım maliyetini de artırmaktadır. Bu yüzden, tesisin ömrü boyunca toplam gideri en aza indirgeyen optimum uzaklık tespit edilmelidir.



1. INTRODUCTION

In future, the world's energy supply must become more sustainable. This can be achieved both by a more efficient use of energy and by relying on renewable sources of energy, particularly wind, hydropower, solar and geothermal energy. Air pollution is becoming a significant environmental concern in the most countries. Achieving solutions to environmental problems that we face today requires long-term potential actions for sustainable development. In this regard, renewable energy resources appear to be one of the most efficient and effective solutions. For the governments or societies to attain sustainable development, much effort has to be devoted to utilizing sustainable energy resources in terms of renewable energies, (Wood et al, 2010). In recent decades, energy consumption for building sector has increased in multifold around the world. Efforts are being made to develop alternate energy sources for meeting the demand of building heating and cooling loads. One of the best alternate ways is the use of ground source energy, which is green and sustainable. This energy can be utilized using GSHP system, which is well established in Western and European countries for space heating applications, (Bakirci, 2010). GSHP systems contain two parts, GHEs and heat pump.

GHEs use underground soil as a heat sink or source. When water flows through pipes, heat is transferred from the water to the earth or from earth-to-water depending upon the temperature of water relative to temperature of earth that remains nearly constant at the annual mean temperature of that place, (Banks, 2008). In some cases, the thermal condition of water coming out from the pipes is such that it can be directly supplied to the space where it is to used, whereas in extreme weather conditions, it needs another stage of processing before becoming acceptable for supplying to the connected space, (Singh, 2013).

To determine the heat transfer in the GHEs with adequate accuracy is a crucial task, and has great impact on sizing and simulating GHE. The design goal is to control the temperature rise of the ground, performance losses between boreholes and the circulating fluid within acceptable limits over the lifetime of the system. A

fundamental task for application of the GSHP technology is to grasp the heat transfer process of a single borehole in the GHE. Heat transfer in a field with multiple boreholes may be analyzed on this basis with the superposition principle, (Yi Man et al, 2012, Omer, 2008). As it is stated in literature, at deeper layers, the ground temperature remains almost constant throughout the year and is usually higher than that of the ambient air during the cold months of the year and lower during the warm months, (Yi Man et al, 2012, Ochsner, 2007). GSHP systems use some electricity to extract heat from the ground and deliver to the space to be heated, thus they indirectly contribute less greenhouse gas generation than the conventional heating systems, (Ozgener and Hepbasli, 2005, Trillat-Berdal et al, 2006).

In many developing countries, in the absence of GSHP, conventional electric resistance heaters are used for space heating in winter and air conditioners for space cooling in summer. With increase in average temperature of earth due to global warming, the need for space cooling systems in summer season is augmented, resulting in significant consumption of centrally generated electricity, (Fan et al, 2008).

Hence, there is an urgent need to find alternative systems for the present air conditioners and heaters. GSHP will be a viable solution as it can be used for both heating and cooling purpose with lesser electricity consumption and with an indirect benefit of reduction in greenhouse gas emissions, (Ozgener and Hepbasli, 2005 ,Trillat-Berdal et al, 2006).

In general, when a GSHP system is designed to operate for heating mode, it will produce higher COP during heating operation. In order to save electricity input to the GSHP system operating both in heating and cooling modes, the system parameters have to be optimized to achieve a higher COP. The influencing parameters of GSHP on the COP can be classified into four groups (Figure 1.1) (Sivasakthivel et al, 2014): GHE parameters, heat pump parameters, ground parameters and climate and distribution parameters. Optimizing these parameters to get high performance is an important aspect in the performance analysis of GSHP systems. With regard to optimization of GHE parameters, few research works have been published, (Rabin and Korin, 1996, Congedo et al, 2012).

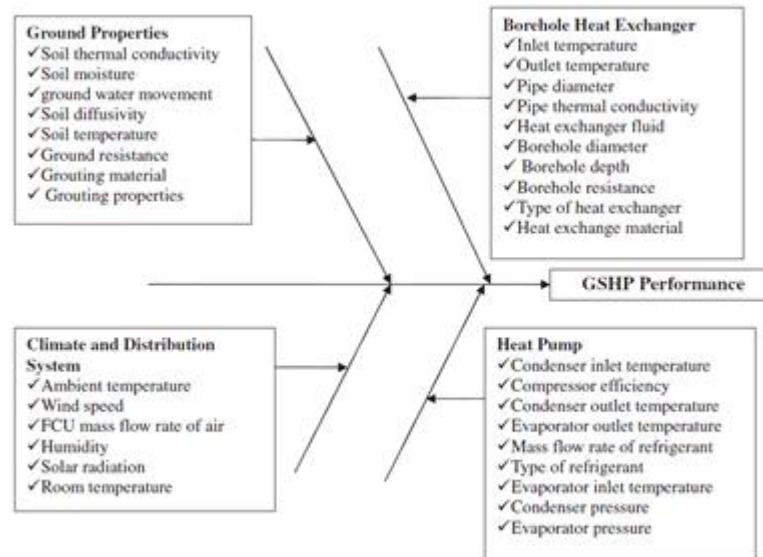


Figure 1.1: Cause and effect diagram for GSHP system (Sivasakthivel et al, 2014).

1.1 Purpose of Thesis

In large-scale GSHP applications, more than one GHE is needed. Optimizing difference between these GHEs plays an important role in GSHP performance. In addition, different parameters highly affect the efficiency of GSHP. One of the most important GHEs is helix one. The purpose of this thesis is to optimize different parameters that are affecting helix GHE performance such as distance between GHEs, pitch length and major diameter of GHEs numerically and experimentally.

1.2 Literature Review

During the last decade, number of investigations has been conducted by some researchers in the design, modeling and testing of GSHP. These studies are mostly related to GHEs design. However, there are few studies in literature just based on helix GHEs.

Rabin and Korin (1996) modeled the helical pipe with a series of horizontal rings with a constant pitch between them and they solved this model by means of finite difference method; they also developed mathematical model for thermal analysis of a helical heat exchanger for long-term thermal energy storage in soil for use in arid zones.

Congedo et al. (2012) carried out Computational Fluid Dynamics (CFD) simulations in order to investigate the horizontal configuration of a helical GHE (Figure 1.2). Their work focused on comparing this set-up with linear and slinky ground heat exchangers during both the winter and summer in the typical climatic conditions of South Italy. In this work, a comparative analysis of two types of horizontal ground heat exchangers, to be coupled with water to water heat pumps, had been performed. For each type ground heat exchanger water velocity and ground thermal conductivity is varied in order to investigate the performance of ground heat exchanger. The heat exchangers were simulated under different operating conditions. Water mass flow rate was set at three different levels (0.25 kg/s, 0.50 kg/s, 1.00 kg/s). The most important parameter that affect the performance of the system was the thermal conductivity of the ground around the heat exchanger. The velocity of the heat transfer fluid inside the pipe was another key factor. The depth of installation of the horizontal ground heat exchangers did not affect the performance. The helical heat exchanger arrangement show the best performance.

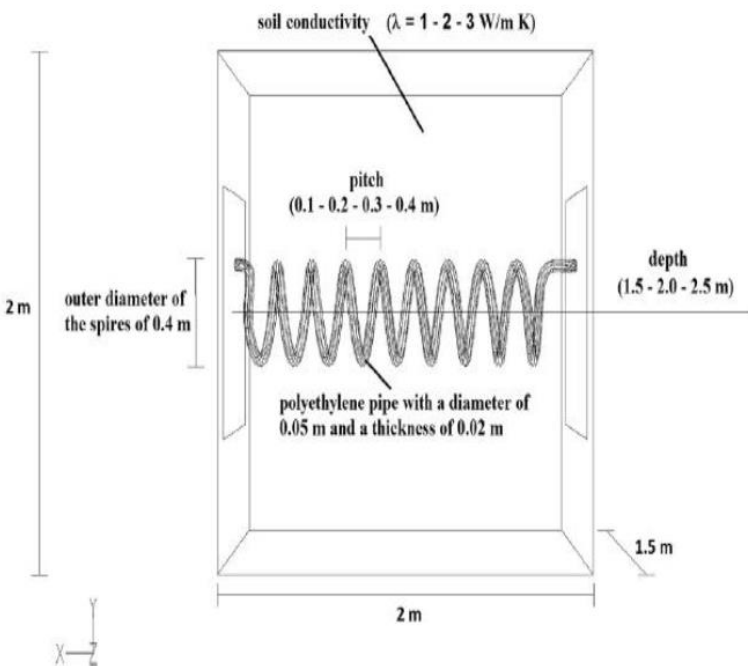


Figure 1.2: Helical horizontal ground heat exchanger configuration considered in the simulations by Congedo et al (2012).

Zarrella et al (2013) investigated the thermal performance of helical and triple U pipes that uses n-U-tubes inside a bore and takes into account axial heat conduction in the ground and the borehole, as well as the borehole's thermal capacitance.

Cui et al (2011) worked on the transient heat conduction around the buried spiral coils which could be applied in the ground-coupled heat pump systems with the pile foundation as a geothermal heat exchanger. They give explicit analytical solutions for the temperature response by means of the Green's function theory and the image method (Figure 1.3).

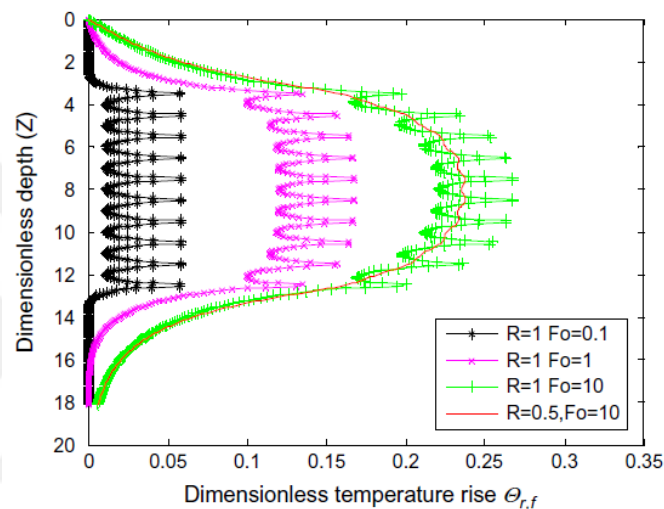


Figure 1.3: Temperature profiles along the three helix GHE with different Fourier number (Fo) obtained by Cui et al (2011)

Park et al (2015) discussed various types of ground heat exchanger and stated that temperature at a certain depth in the ground remains nearly constant throughout the year. The ground capacitance can be regarded as a passive means of heating and cooling of buildings. Vertical borehole heat exchangers were drilled to different depths of 20–300 m with different diameters of 10–15 cm. It has been found that performance of ground heat exchanger is effected by length of bore hole, U-tube shank spacing, thermal conductivity of the grout and diameter of the pipe.

Ascione et al (2011) investigated the energy performances of an earth-to-air heat exchanger for an air conditioned building for both winter and summer conditions. The performance of the systems have been analyzed for different boundary conditions such as the type of soil, pipe material, pipe length, depth, velocity of the air crossing the pipe, ventilation air flow rates. Normally, the soil temperature at a

depth of 5 to 8 m under the ground level remains almost constant throughout the year.

Esen et al (2009) presented a model to find out the temperature distribution of U tube borehole for ground coupled heat exchanger system according to borehole depth. In this study vertical drilling of bore was carried for three different depth as 30, 60 and 90 meter. The best performance of the system was obtained at a depth of 90 meter but optimum depth is about 60 meter. In this study experimental result compared with simulation result which was performed by commercial code ANSYS . Design length and performance of heat exchanger strongly depend on the thermal conductivity of the backfill material.

Wang et al (2009) investigated that due to ground water flow performance of borehole heat exchanger increased and based on the measurement of the natural ground temperature profile, a theoretical model was presented to estimate the affect of groundwater flow.

Sagia et al (2012) studied that bore hole thermal resistance in ground heat exchanger is affected by parameters such as geometrical attributes of heat exchanger in the bore hole, pipes properties and grout thermal conductivity. Borehole thermal resistance decreased as shank spacing between GHE pipes increased, a rise in grout's thermal conductivity lead to a fall of borehole resistance and the slighter wall pipe enabled a bigger heat transfer rate between the heat carrier fluid and the ground. A small value of borehole thermal resistance is desirable in order to achieve a high performance of ground heat exchanger. schematic view of borehore heat exchanger is given in Figure 1.4.

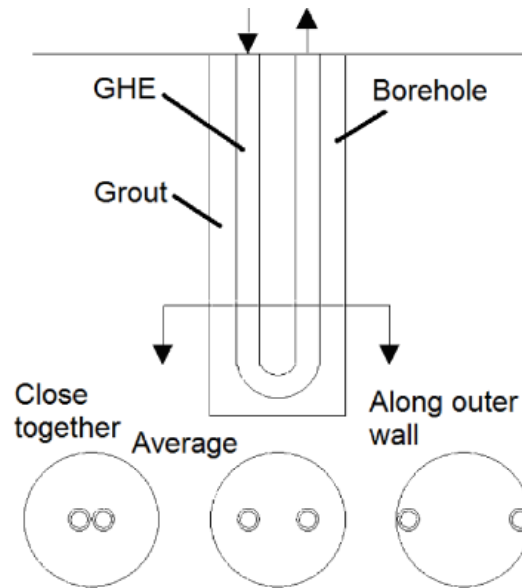


Figure 1.4: Vertical GHE and configurations (Sagia et al, 2012)

Koohi-Fayegh and Rosen (2012) study the heat flows in the soil surrounding boreholes in the long run. They present a numerical model for the region outside the borehole and assume a periodic heat flux at the borehole wall (Figure 1.5).

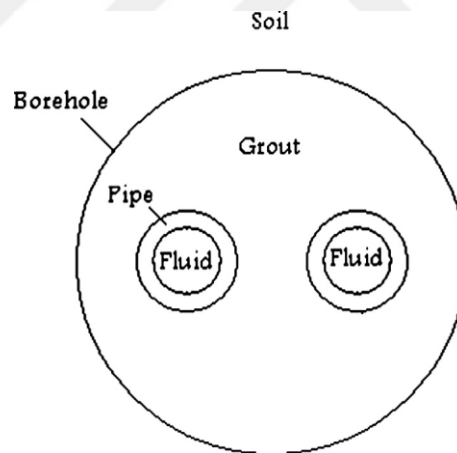


Figure 1.5: Cross-section of a vertical GHE. The fluid is ascending in one pipe and descending in the other,(Koohi-Fayegh and Rosen, 2012).

Koohi-Fayegh and Rosen (2014) also use an analytical solution to the heat transfer problem inside the borehole to evaluate the temperature of the circulating fluid along the borehole length. This solution is then used to calculate the heat delivery/removal along the borehole caused by the temperature difference between the circulating fluid and the borehole wall temperature. The heat delivery/removal calculated from the model inside the borehole is implemented as the heat boundary condition in the

analytical line source with finite length as well as in a three-dimensional finite volume model.

Miyara et al (2011) studied several types of ground heat exchangers (GHEs) installed in a steel pile foundation around the bore hole, including double-tube, U-tube, and multi-tube GHEs. The performance of GHEs was investigated in the cooling mode with flow rates of 2, 4, and 8 lt/min. The temperatures of the inlet and outlet of circulated water were also measured to calculate the heat exchange rate. The double-tube had the highest heat exchange rate than multi-tube and U-tube GHEs.

Lazzari et al (2010) investigated the long-term performance of double U-tube BHE (borehole heat exchanger) fields by finite element simulations, performed through the software package COMSOL Multiphysics. They also analyzed different configurations of boreholes. Four different distances between adjacent boreholes and two values of the ground thermal conductivity are considered in their study.

Khalajzadeh et al (2011) discussed a variable undisturbed ground temperature profile of a vertical ground heat exchanger and the presence of underground water flow is not considered. A full three dimensional computational fluid dynamics simulation with 3.5 % error was performed using the CFD software. The objective of this paper was to quantify the total heat transfer efficiency and heat exchanger efficiency of vertical ground heat exchanger. As the depth of borehole is increased, the heat exchanger efficiency is increased but the total heat transfer efficiency is decreased. Optimization was performed with the conditions which are heat exchanger efficiency and total heat transfer efficiency.

1.3 Present Study

In this thesis, time variation of HTR values of vertical helix GHEs is numerically modelled and available experimental data at Energy Institute of Istanbul Technical University are used for the validation of the model. Effects of distance between GHEs, pitch length and major diameter on their HTR values are analyzed.

Contents of this study is as follows: a literature survey is presented in Chapter 1. Chapter 2 gives general information about heat pumps and GSHP systems. Chapter 3 presents the experimental system and measurement devices as well as and the results of the experiments. Chapter 4 contains simulation models of different configuration

of vertical helix GHE. Results of numerical solution such as time variation of HTR value, temperature distribution in soil, effect of L_p and D on HTR value are also given in this chapter. Chapter 5 gives the conclusion and analysis of the system performance.



2. GROUND SOURCE HEAT PUMP

2.1 Heat Pump

Heat is transferred from high-temperature media to low-temperature media without requiring any device. However, to perform the reverse process, some devices are needed. Heat pumps and refrigerators are devices that receive heat from a lower temperature reservoir and reject it to a higher temperature reservoir. Heat pump has the same cycle with a refrigerator that is commonly used in residences. The difference in between a refrigerator and a heat pump is only the purpose. Refrigerators are intended for cooling a selected space by extracting heat at lower temperature. If desired effect is to heat the space, heat is discharged at higher temperature in heat pumps, (Cengel and Boles, 2011).

A heat pump can either extract heat from a heat source and reject heat to air and water at a higher temperature for heating, or provide refrigeration at a lower temperature and reject condensing heat at a higher temperature for cooling. During summer, the heat extraction, or refrigeration effect, is the useful effect for cooling in a heat pump. In winter, the rejected heat provides heating in a heat pump, (Ingley et al, 2005).

Heat pumps provide both energy-efficient and cost-efficient solution to the demand for heating. The most important advantage of this type of heating system is that more energy can be available for space heating than the work required to operate a heat pump. In fact, modern electrical heat pumps can achieve performance factors (coefficient of performance, COP) between 3.5 and 5.5. This means that for every kWh power consumption, 3.5 to 5.5 kWh heating energy can be created (Cengel and Boles, 2011). Addition to this high performance advantage, causing less pollution, the ability to make both heating and cooling and the feasibility for industrial applications have increased the popularity of heat pumps.

2.1.1 Overview

The heat pump uses the concepts of the vapor compression cycle to transfer heat from one source to another. Heat pumps exchange energy between the conditioned interior space and either the ground or the air. For the purposes of this study, only ground-source heat exchange is considered. In heating mode, the coil in the ground loop becomes the evaporator, while the coil in the conditioned interior of the home becomes the condenser, thus absorbing the heat from the refrigerant. The refrigerant absorbs heat from the water in the ground-source loop, is compressed by the compressor, and sent to the evaporator. The refrigerant then rejects heat to the space where it is distributed throughout the home. In cooling mode, the coils are reversed with the conditioned space being the evaporator and the ground source loop becoming the condenser. Figure 2.1 shows the simplified heat pump system with the primary heat and work interactions between the cycles and surroundings. The box represents the control volume defined for the vapor compression system. The “hot” and “cold” bodies represent the thermal reservoirs and the arrows indicate the rate of heat transfer \dot{Q} to and from the system as well as the total power \dot{W}_{cycle} required for the cycle.

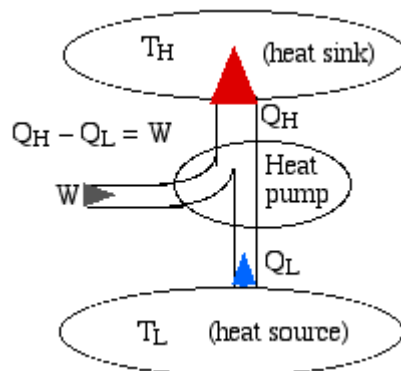


Figure 2.1: Simplified model of a heat pump system.

2.1.2 The reversed Carnot cycle

The Carnot cycle is a totally reversible cycle and it is composed of two reversible isothermal and two reversible adiabatic (isentropic) processes. The theoretical heat engine that operates on the Carnot cycle is called the Carnot heat engine and the reverse cycle of it is called the Carnot refrigeration cycle (Çengel and Boles, 2011).

A heat engine receives heat from high temperature reservoir and produces work by rejecting that heat to low temperature reservoir. Maximum theoretical work that a heat engine can produce is achieved by Carnot cycle. Consequently, the maximum possible efficiency of a cycle can be obtained from the Carnot cycle between same temperature reservoirs according to the Carnot principles. Figure 2.2 shows the P-v and T-s diagrams of a reversed Carnot cycle.

The Carnot vapor compression cycle is the theoretical system that describes all heat pump cycles. All processes in the Carnot cycle are assumed to be internally reversible (i.e., no losses), as are the isothermal heat transfer processes. The expansion valve is replaced by a turbine because of the assumed reversibility. The components for this cycle are shown in Figure 2.3.

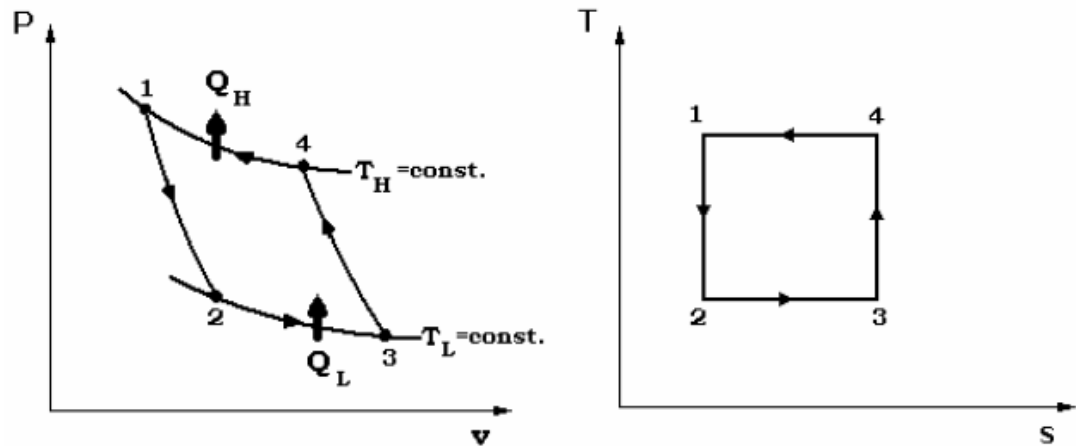


Figure 2.2: P-v and T-s diagrams of a reversed Carnot cycle.

The four reversible processes are as follows:

- a) 1-2 Reversible adiabatic (isentropic) expansion: The temperature of the working fluid that is at T_H temperature drops to T_L temperature isentropically.
- b) 2-3 Reversible isothermal heat absorption: Heat is transferred isothermally from the low-temperature source at T_L temperature to the working fluid in the amount of Q_L .
- c) 3-4 Reversible adiabatic (isentropic) compression: The working fluid is compressed isentropically by doing work on the system. The temperature of the fluid increases from T_L temperature to its initial T_H temperature.

- d) 4-1 Reversible isothermal heat rejection: The working fluid rejects heat at constant T_H temperature to the high-temperature reservoir in the amount of Q_H .

A work done on the system is needed to keep the temperature of the space above the 4 atmospheric temperature. According to the Clausius statement in thermodynamics, *it is impossible to construct a device that operates in a cycle and produces no effect other than the transfer of heat from a lower temperature body to a higher temperature body*. That is, heat cannot be transferred from a lower temperature medium to a higher temperature medium without an input of work.

The coefficient of performance of a heat pump is the ratio of the desired output Q_H to required input W_{net} ($Q_H - Q_L$) by definition:

$$COP_{HP} = \frac{\text{desired output}}{\text{required input}} = \frac{Q_H}{Q_H - Q_L} = \frac{Q_H}{W_{in}} \quad (2.1)$$

Since energy reservoirs are characterized by their temperatures, the coefficient of performance of a reversible heat pump (Carnot heat pump) is a function of the temperatures only and becomes:

$$COP_{HP,Carnot} = \frac{T_H}{T_H - T_L} \quad (2.2)$$

This is the highest value that a heat pump operating between the temperatures limits of T_L and T_H can have (Çengel and Boles, 2011).

2.1.3 The ideal vapor compression refrigeration cycle

The working fluid (refrigerant) is vaporized completely before compression on the ideal vapor compression refrigeration cycle since the existence of liquid in vaporized refrigerant entering a compressor can damage the valves. The turbine on Carnot cycle is replaced with a throttling device, such as expansion valve or capillary tube. This cycle is the most widely used cycle for refrigerators, air conditioning systems and heat pumps. Schematic and T-s diagrams of an ideal vapor compression refrigeration cycle are shown in Figure 2.3. It consists of four processes (Çengel and Boles, 2011):

- a) 1-2 Isentropic compression in compressor

- b) 2-3 Constant pressure heat rejection in condenser
- c) 3-4 Throttling in an expansion device
- d) 4-1 Constant pressure heat absorption in an evaporator

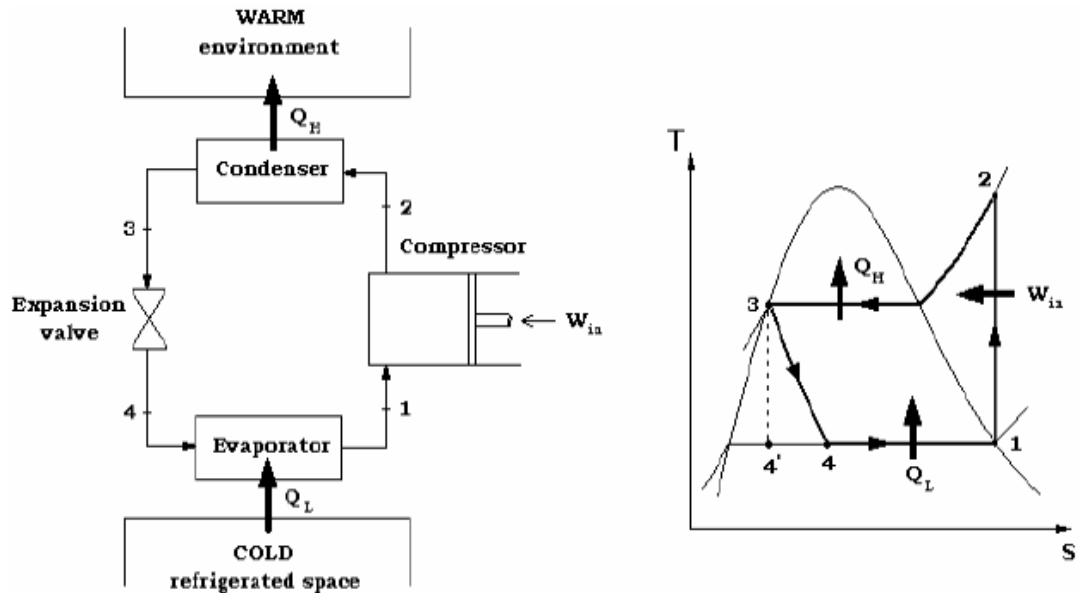


Figure 2.3: Schematic and T-s diagram for the ideal vapor compression refrigeration cycle (URL-2) .

The refrigerant enters the compressor at state 1 as saturated vapor with low pressure and temperature and is compressed isentropically to the condenser pressure. The temperature of the refrigerant increases during this isentropic compression process to well above the temperature of the surrounding medium, such as atmospheric air. Then the refrigerant enters the condenser as superheated vapor at state 2 and leaves as saturated liquid at state 3 by rejecting heat to high temperature medium (the surroundings).

The pressure of the saturated liquid refrigerant at state 3 drops to the evaporator pressure by passing through an expansion valve or capillary tube. The temperature of the refrigerant drops below the temperature of the refrigerated space during this process. The refrigerant enters the evaporator at state 4 as a low-quality saturated mixture and it evaporates completely by absorbing heat from the refrigerated space. The refrigerant leaves the evaporator as saturated vapor and enters the compressor. Therefore, the cycle is completed (Çengel and Boles, 2011).

The ideal vapor compression refrigeration cycle is not an internally reversible cycle because it involves an irreversible throttling process.

Another diagram frequently used in the analysis of vapor compression refrigeration cycle is the P-h diagram, as shown in Figure 2.4.

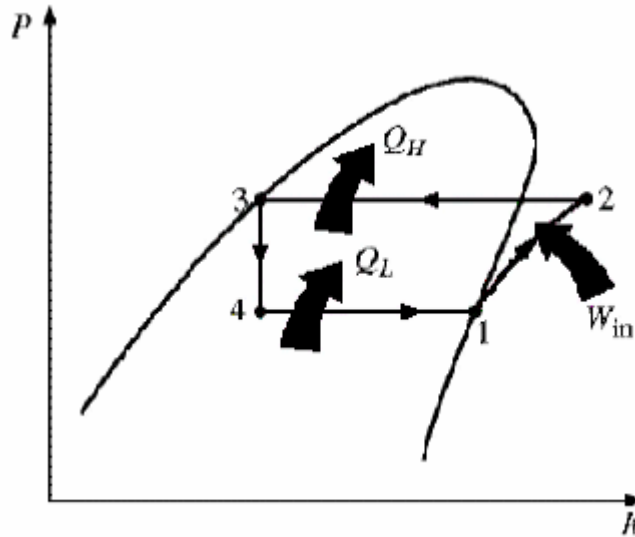


Figure 2.4: P-h diagram of ideal vapor compression refrigeration cycle.

The coefficient of performance of heat pumps operating on the ideal vapor compression refrigeration cycle can be expressed as:

$$COP_{HP,Carnot} = \frac{Q_H}{W_{net,in}} = \frac{h_2 - h_3}{h_2 - h_1} \quad (2.3)$$

where, h denotes enthalpy values of corresponding states, q_h is heat rejected at condenser and $w_{net,in}$ is work input to the system.

2.1.4 Actual vapor compression refrigeration cycle

Actual vapor compression refrigeration cycle deviates from the ideal cycle due to irreversibilities. Two common reasons for irreversibilities are fluid flow, which causes pressure drops and heat transfers. The T-s diagram of an actual vapor compression refrigeration cycle is shown in Figure 2.5.

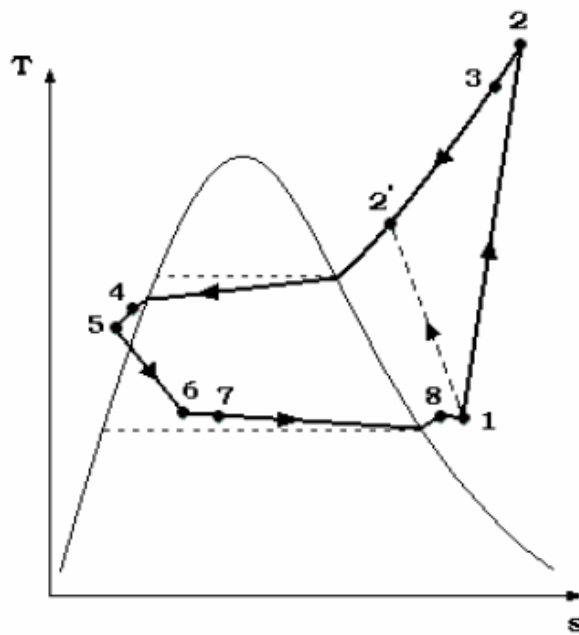


Figure 2.5: T-s diagram of the actual vapor compression refrigeration cycle.

The refrigerant enters the compressor as slightly superheated instead of saturated vapor. Furthermore, the piping between the evaporator and the compressor is very long, thus a significant heat transfer from the surroundings and a pressure drop caused by fluid friction occur along the piping. There is also a pressure drop in the evaporator. These three deviations from the ideal cause an increase in specific volume of the refrigerant and thus an increase in the power requirements to the compressor.

The compression process, which is assumed to be isentropic in the ideal cycle, may have an increase or decrease in entropy. At the compressor inlet, the refrigerant has lower temperature than the compressor cylinder wall and therefore heat is transferred to the refrigerant. In the same way, heat is transferred from the refrigerant at the compressor exit because the temperature of the refrigerant is higher than the compressor temperature. Therefore, an increase in entropy occurs at the beginning of the compression and a decrease in entropy at the end of it.

It is difficult to realize a constant pressure process at the condenser since there is a pressure drop. Therefore, the temperature of the refrigerant becomes lower than the saturation temperature and the refrigerant enters the throttling valve as subcooled. A pressure drop also occurs in the piping between the condenser and the throttling valve.

Overall COP of a system that includes more applications than a heat pump like solar assisted heat pump can be calculated by following relation:

$$COP_{HP} = \frac{Q_H}{W_{comp} + W_{fan} + W_{others}} \quad (2.4)$$

Log-h diagram of an actual vapor compression cycle is shown in Figure 2.6.

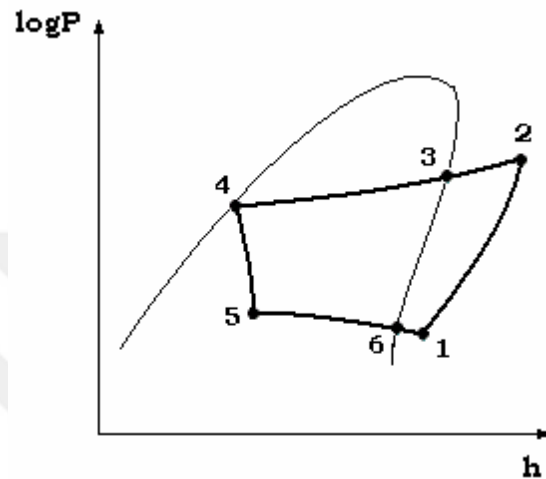


Figure 2.6: Real process of a vapor compression heat pump cycle.

The changes of states, which deviate from ideal process, can be described as follows:

- a) 1-2 Compression with a variable polytropic exponent
- b) 2-3 Heat output with loss of pressure due to friction
- c) 3-4 Heat output by condensation with loss of pressure
- d) 4-5 Expansion with heat input
- e) 5-1 Heat input with loss of pressure and superheating

2.1.5 Heat sources

Three common sources widely use in heat pump systems. Air, soil and water. An ideal heat source is inexpensive, abundant and it has a temperature as high as possible. The difference should be small between the desired temperature and the temperature of available heat source. In addition, the heat transfer medium should not affect the heat exchange equipment chemically and physically (Singh, 2013) .

2.1.5.1 Air

Air is the most common source in practice and it offers the possibility of a substantially universal heat source. However, there are a number of problems associated with its use as a heat source although air is free and widely available. Many localities experience not only wide fluctuations in air temperature, but also the temperature as the heating requirements increase. This will adversely affect the coefficient of performance and the size of the refrigeration system. In the cooler and more humid climates, some residual frost tends to accumulate on the outdoor heat transfer coil (evaporator) as the temperature falls below the 2-5 °C range, leading to a reduction in the capacity of the heat pump. As the heating load is greatest at the lowest temperature, a supplementary heating source is required. This device could be an existing oil, gas or electric furnace or electric resistance heating; the latter is usually part of the heat pump system (Sporn et al, 1947).

2.1.5.2 Soil

Soil is very suitable heat source because of its high and constant temperature, availability and storage capacity. Generally, the heat can be extracted from pipes laid horizontally or sunk vertically in the soil. The latter system appears to be suitable for larger heat pump systems.

Due to the removal of heat from the soil, the soil temperature may fall during the heating season. Depending on the depth of the coils, recharging may be necessary during the warm months to raise the ground temperature to its normal levels. This can be achieved by passive (e.g., solar irradiation) or active means, (Sauer and Howell, 1983).

2.1.5.3 Water

Because of its high heat capacity and good heat transfer properties, water is the best heat source. Water from wells, lakes, rivers, and waste waters meets to requirements. Water-source units are common in applied or built-up installations where internal heat sources, heat or cold reclaim is possible. In addition, solar or off-peak thermal storage systems can be used (Sporn et al, 1947).

Ground water, i.e. water at depth of up to 80 meters, is available in most areas with temperatures generally in the 5-18 °C range. One of the main difficulties with these

sources is that often the water has a high dissolved solids content producing fouling or corrosion problems with heat exchangers (Sauer and Howell, 1983).

Water-to-air heat pump uses water as a heat source and uses air to move the heat to or from the conditioned space. Almost any water can be used as the source: river water, lake water, ground or well water, waste water, and so on.

2.2 Ground Source Heat Pump Systems

Ground source heat pumps, often referred to as geothermal heat pumps, are recognized to be heating, cooling, and water-heating systems. They provide high levels of comfort, offer significant reductions of electrical energy use and demand, have very low, levels of maintenance requirements, and are environment friendly. A ground source heat pump is a heating and cooling system that transfers heat to or from the ground, using the ground as a heat sink in the summer and heat source in the winter. A ground source heat pump can be significantly more energy efficient than conventional air source heat pump. The heat source of a GSHP is the ground. The heat is taken from the ground by a borehole heat exchanger (there is a lot of different kind of BHEs: U-pipe, helical shaped...). The heat is then transported from the ground to the evaporator of the heat pump and supply the evaporator energy

.(Ascione et al, 2011). The schematic view of GSHP is shown in Figure 2.7.

Ground source heat pumps have some main advantages over conventional air source heat pumps as:

- a) They consume less energy to operate.
- b) They are more stable energy source than air.
- c) They do not require supplemental heat during extreme low outside temperature.

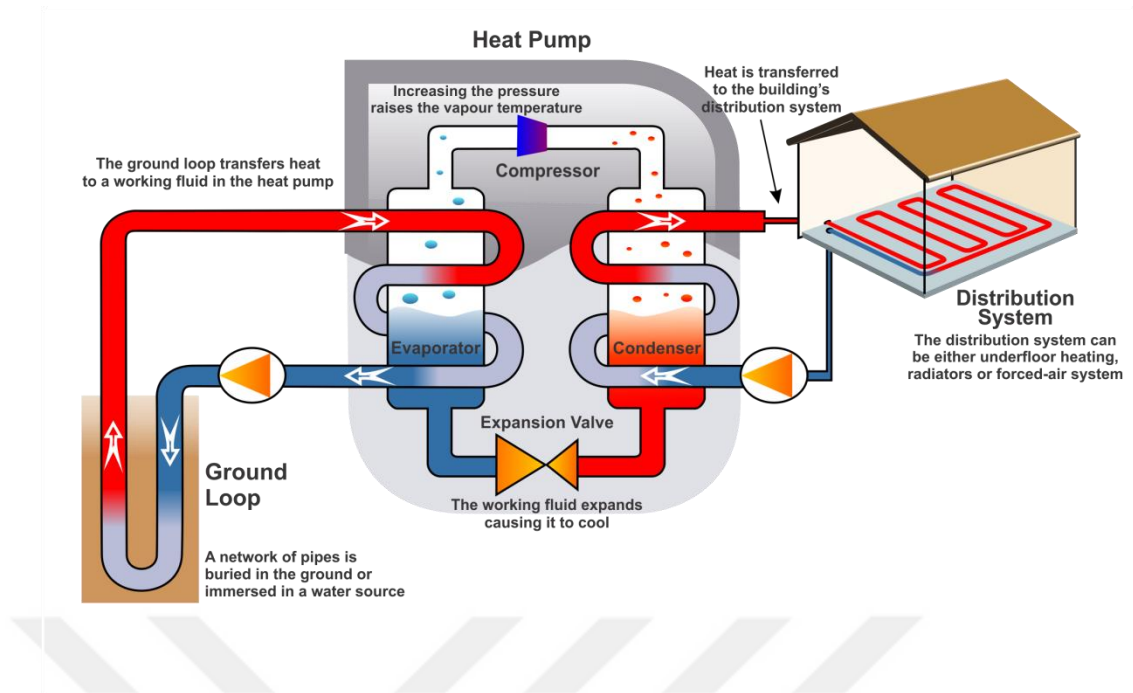


Figure 2.7: GSHP Schematic view.

2.2.1 Ground heat exchanger

Ground heat exchangers use underground soil as a heat sink or source. When water flows through pipes, heat is transferred from the water to the earth or from earth-to-water depending upon the temperature of water relative to temperature of earth that remains nearly constant at the annual mean temperature of that place. In some cases, the thermal condition of water coming out from the pipes is such that it can be directly supplied to the space where it is to be used, whereas in extreme weather conditions, it needs another stage of processing before becoming acceptable for supplying to the connected space. Ground temperature below a certain depth remains relatively constant throughout the year because temperature fluctuations at the surface of the ground are diminished as the depth of the ground increases because of the high thermal inertia of the soil. Therefore ground temperature is always higher than that of the outside environment in winter and is lower in summer at a sufficient depth. The difference in temperature between the outside environment and the ground can be utilized as a preheating means in winter and pre-cooling in summer by operating a ground heat exchanger. Efficiency of a heat pump is higher than conventional natural gas or oil heating systems, a heat pump may be used in winter to extract heat from the ground and pump it into the conditioned space. In summer, the process may be reversed and the heat pump may extract heat from the

conditioned space and send it out to a ground heat exchanger that warms the relatively cool ground. A ground source heat pump extracts heat from the ground – whose temperature will be warmer than the air in winter (and cooler than the air in summer). Therefore ground heat exchangers are more efficient than air source heat pumps, especially in the coldest weather when they are most needed. Ground heat exchangers generate very little noise and should last for many years with minimal servicing. Ground heat exchanger are the system that is simple to use and easy to maintain. In addition, since the system takes care of both heating and cooling. Geothermal energy is a form of clean energy because using it doesn't emit any type of pollutions (Banks, 2008).

2.2.1.1 History

The ground heat exchanger was described by Lord Kelvin in 1853 and developed by Peter Ritter von Rittinger in 1855 (Url-1). After experimenting with a freezer and Robert Webber built the first direct exchange ground heat exchanger in the late 1940s. The first successful project was installed in the Commonwealth Building (Portland) in 1946 and has been designated a national historic mechanical engineering landmark by ASME. This technology becomes popular in Sweden in the 1970, and has been growing slowly. Open loop systems controlled the market until the development of polybutylene pipe in 1979 made closed loop systems economical. Since 2004, there are over a million units installed worldwide providing 12 GW of thermal capacity. 80,000 units are installed in the US every year and 27,000 in Sweden every year (Url-2).

2.2.1.2 Need of ground heat exchanger

Factors like rising electricity prices and the environmental factors have forced us to look for cheaper and cleaner alternatives to various applications. Water heating and cooling is one such device that heavily consumes electricity and its emissions are detrimental to the environment. The high current requirements of the water heating and cooling require the installation of the high capacity electric cables. Also, because of the intermittent starting and stopping of the air-conditioners the installed capacity of the electricity has to be much higher than required for the actual running. Moreover, the gap in the demand and supply of the electricity in our country limits the suitability of the water heating and cooling. One of the alternatives that can

address the above mentioned concerns and the most promising energy resources available to man is geothermal energy. It is a form of clean energy because using it doesn't emit any type of pollutions, and renewable energy because the heat within the ground goes around in a cycle so we are assured that there will always be heat available to us. Geothermal energy is mainly used in electricity production. Geothermal energy power plants are becoming a popular alternative to plants that run on fossil fuel. Geothermal energy is also used for heating, especially in many localities in Iceland, Turkey, and the United States. On a smaller scale, geothermal energy is using ground heat exchanger for heating and cooling purpose (Singh, 2013).

2.2.1.3 Mechanism of heat transfer

Ground heat exchangers use underground soil as a heat sink or source. Ground temperature below a certain depth remains relatively constant throughout the year because temperature fluctuations at the surface of the ground are diminished as the depth of the ground increases because of the high thermal inertia of the soil. When water flows through pipes, heat is transferred from the earth to the water or from the water to the earth depending upon the temperature of water relative to temperature of earth that remains nearly constant at the annual mean temperature of that place (Florides and Kalogirou, 2007). Heat is transferred in the ground by two ways, convection and conduction.

Convective heat transfer: Convection is the transfer of heat from one place to another by the movement of fluids (liquid and gas). Convection is a dominant form of heat transfer in fluids. The term convection can refer to transfer of heat by fluid movement. The process of transfer of heat from a solid to a fluid or from fluid to surface requires not only transfer of heat by bulk motion of the fluid, but also by conduction of heat through the still boundary layer next to the solid. Thus, convection is a process with a moving fluid requires both advection and diffusion of heat. The convection heat transfer depends upon the type of fluid, flow velocity, the area of contact and the temperature gradient. This is mainly classified as natural or free convection and forced convection. Natural convection results from the variations of the density due to the temperature gradient in the fluid. On the other hand, forced

convection is artificially induced by means of some external source like fan, blower or pump.

Conduction heat transfer: Whenever a temperature gradient exists in a solid medium, heat will flow from the higher-temperature to the lower-temperature region. The rate at which heat is transferred by conduction, q_k , is proportional to the temperature gradient times the area A through which heat is transferred:

$$q_k = -kA \frac{dT}{dx} \quad (2.5)$$

In this relation, $T(x)$ is the local temperature and x is the distance in the direction of the heat flow. Physical property k is the thermal conductivity of the medium (Kreith et al, 2011).

The soil is considered as the main medium in this thesis. Heat is generally transferred by conduction through the pipes in dry conditions. Having good knowledge about thermal conductivity of soil help us to determine the q_k as well as possible. Thermal conductivity of soil differ in the range of $1.5-3.5 \text{ Wm}^{-1} \text{ k}^{-1}$ based on the properties of it (Banks, 2008).

There are two types of ground source heat systems: open-loop and close-loop systems.

2.2.2 Open Loop systems

Open-loop systems are those where we physically abstract water from a source, this can be a river, the sea or a lake.(Figure 2.8) In the context of thermogeology, however, we are primarily concerned with groundwater abstracted from springs, dug wells, drilled boreholes or flooded mines. Heat is extracted from this flux of pumped water or in cooling mode dumped into it. In cooling mode, we do not necessarily need to use a heat pump (Banks 2008).

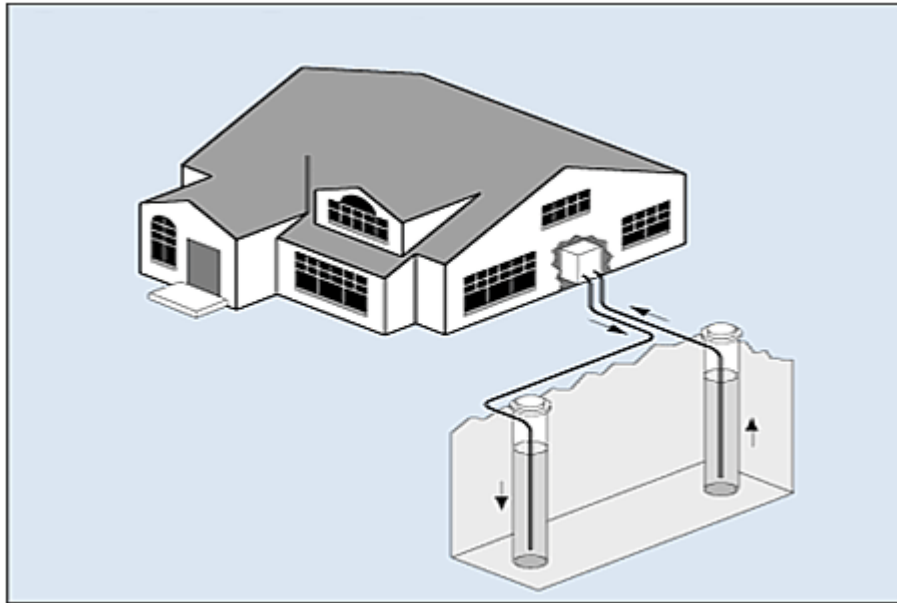


Figure 2.8: Open-loop system (Banks, 2008)

2.2.3 Closed Loop systems

There is another way to extract heat from the ground that does not require any water to be abstracted or re-injected at all. Such schemes are called closed-loop schemes and they can be constructed practically anywhere in granites, clays, waste tips, permafrost or abandoned mines. Closed loop schemes are of two types: direct circulation and indirect circulation. Direct circulation schemes were more common in the early years of GSHP systems, although some companies are still installing them today, indirect circulation schemes have become far more widespread than direct circulation schemes in today's European GSHP market (Banks, 2008).

2.2.3.1 Horizontal closed loops

One of the cheapest forms of indirect closed loop scheme is the horizontal closed loop, installed in a trench (Figure 2.9). The optimal depth for such a trench is regarded as 1.2-2 m. This depth is:

- a) One that can be practically excavated using a mechanical excavator;
- b) Deep enough to provide a sufficient thermal storage to support a heating scheme during a winter, a reasonable soil moisture content and to isolate the loop from the worst winter frosts;
- c) Shallow enough to allow solar and atmospheric heat to penetrate and replenish the thermal storage around the loop during the summer months.

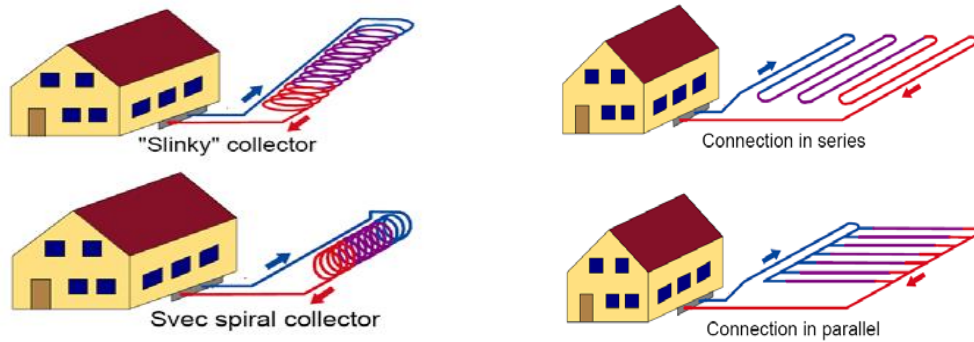


Figure 2.9: Horizontal closed loops GHEs (URL-2)

2.2.3.2 Pond and lake loops

Coils of polyethylene pipes can also be installed in deep ponds or lakes (Figure 2.10). For this to be an appropriate solution, the lake should ideally be at least 3 m deep, to ensure that natural temperature variation at its base are low. The lake should also be large enough, so that the heat extracted by the heat pump does not change the temperature of the lake water by an unacceptable amount.

Figure 2.10 shows heat transfer mechanism in shallow pond GHEs. Different types of heat transfer is also given in this figure.

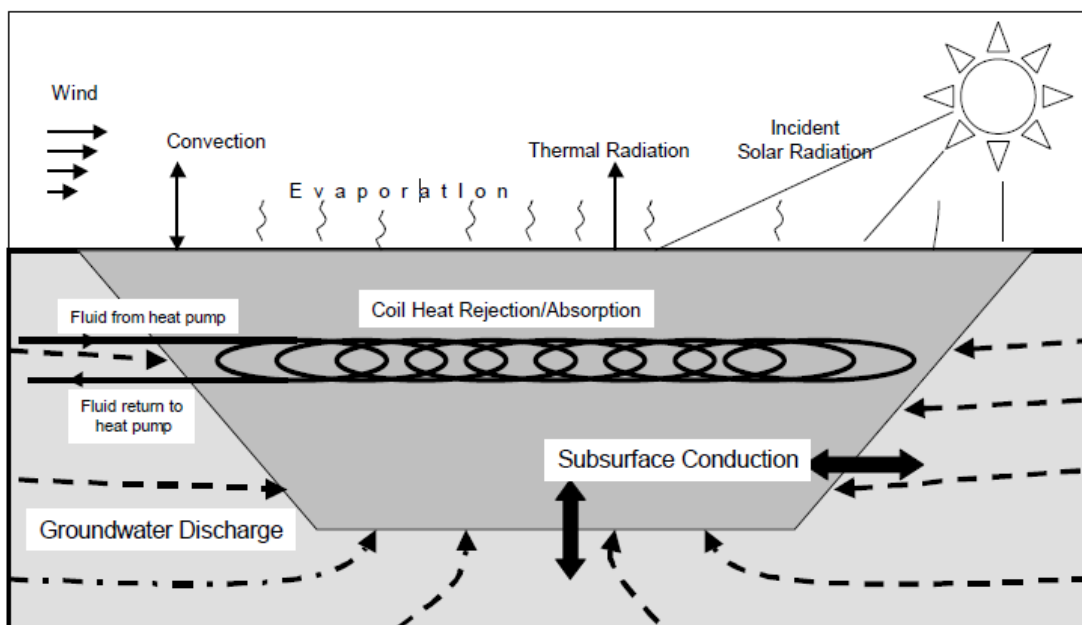


Figure 2.10: Heat transfer mechanisms in shallow ponds (Banks, 2008).

2.2.3.3 Vertical closed loops

If there is a large amount of available space at our development site, horizontal trenched installation may be the cheapest means of installing a ground loop. At many sites, however ground area is at a premium. A far more space efficient means of installing a ground loop array is via vertically drilled boreholes.

Such boreholes are not nearly as sophisticated as the water wells. Although a short length of permanent casing should be installed and grouted in the uppermost section of the borehole to prevent surface contamination entering the subsurface, such boreholes are typically drilled either open-hole or using only temporary casing in loose rocks or sediments.

Two common vertical heat exchangers are U-tube and helical shaped heat exchangers (Figure 2.11). In order to use U-tube heat exchangers the ground should be drilled about 100-200 m. helical shaped heat exchangers are placed in maximum 3 m. thermal behaviors of two heat exchanges were investigated by Zarrella (Zarrella et al, 2013). A helical pipe, rather than U-tubes, is proposed for use in the pile as its technical advantages make it the more effective configuration. The helical-pipe energy pile provided better thermal performance than the triple U-tube configuration in the same conditions.

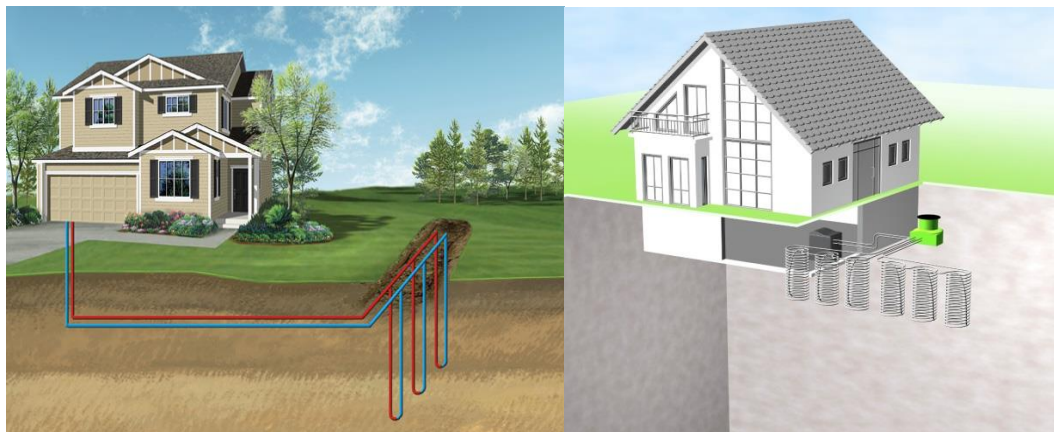


Figure 2.11: Schematic view of U-tube and helical GHEs (URL2)

Figure 2.12 shows the schematic view of different types of closed loop systems.

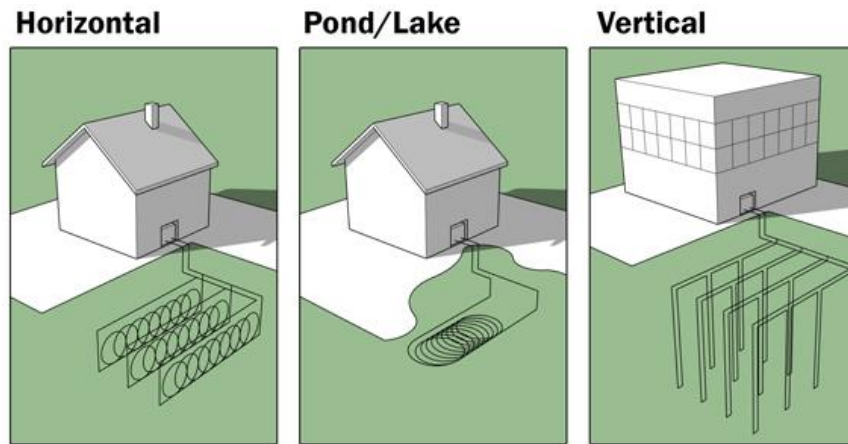


Figure 2.12: Closed-loop systems (Banks, 2008)

2.2.4 The benefits of GSHPs

We can list a host of reasons why GSHPs provide attractive sources of heating and cooling. Firstly, they are visually unobtrusive: a typical water - to - water heat pump is a white box, not unlike a fridge. They can be tucked away in a cellar or a plant room and nobody need know that they are there. Conventional air - conditioning and cooling systems may require large units to be bolted on to the side of buildings or mounted on the roof . Even other environmentally friendly energy sources can have a major visual impact: consider wind turbines, solar thermal panels or photovoltaic arrays mounted on the roofs of buildings. The low visibility of GSHPs can be particularly attractive to those requiring cheap ‘ green ’ energy in a national park or other area where planning regulations restrict visual impact of new developments. The low visibility of GSHPs has a downside as well: wind turbines and solar panels advertise themselves, saying ‘ Look at me; I ’ m a low - carbon household ’ . GSHPs are not immediately obvious; possibly one reason for the initial resistance of the UK market to the technology (Banks, 2008)..

Furthermore, a large office building that is cooled and heated by GSHPs may not need the massive roof - mounted evaporative cooling towers associated with conventional cooling systems. This may have structural implications for the building: it will not have to bear the weight of the cooling towers, possibly saving construction costs. It will also free up roof space for high - value penthouse apartments and offices. GSHPs present a minimal fire hazard and require minimal ventilation. They are also extremely low maintenance and have a long lifetime compared with many fossil fuel boilers. GSHPs produce relatively little noise, if properly mounted in an

insulated cabinet, and can be placed in a household utility room or garage with minimal disturbance. (GSHPs, like fridges, do emit some noise, however. They should probably not be placed in a room that is regularly occupied.) Probably, the most important advantages relating to heat pumps are (1) running cost and (2) environmental impact in terms of CO₂ emissions. Before we proceed, it is important to realise that GSHPs provide a low - CO₂ source of heating, but not usually a zero - CO₂ source.



3. EXPERIMENTAL SETUPS

3.1 Ground Source Heat Pump Test and Research Laboratory

GSHP test and research laboratory has been established in 2012 at Istanbul Technical University Energy Institute. There are some facilities in this laboratory to do some tests and research about GSHP systems. There are six (6) boreholes with different properties. These properties are listed in Table 3.1. Figure 3.1 also shows the view of boreholes in laboratory surroundings. The map of laboratory is given in appendix A.



Figure 3.1: Different boreholes in laboratory

Table 3.1: Properties of different boreholes at Energy Institute of ITU

Number of borehole	Depth [m]	Number of pipes	Pipes Diameter [mm]	Borehole Diameter [mm]	Shank space [mm]
1	50	1-U	32	176	97
2	50	1-U	32	176	97
3	50	2-U	32	176	97
4	100	1-U	32	176	97
5	50	1-U	40	200	120

Also there are some other types of GHE in our laboratory. Slinky, horizontal and vertical helix, horizontal spiral GHE. Figure 3.2 demonstrates vertical helix GHE that placed between 1.5 and 4.5 meter in the ground. Figure 3.3 shows spiral and slinky types with their physical properties (Table 3.2).



Figure 3.2: Vertical helix GHE

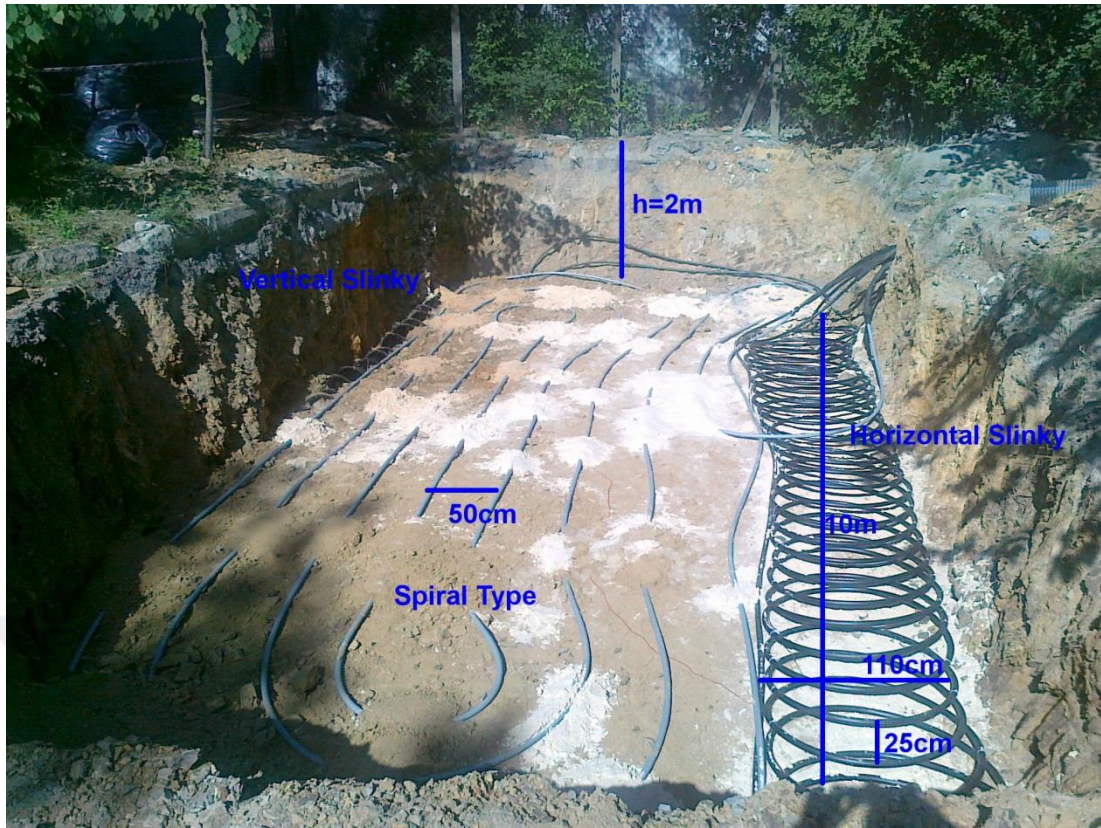


Figure 3.3: Spiral and slinky GHE

Table 3.2: Different types of GHE at ITU Energy Institute

Type of GHE	Length of pipe [m]	Depth from the surface [m]	Pipes Diameter [mm]
Horizontal slinky	100	2	32
Vertical slinky	100	2	32
Horizontal helix	40	1.5	25
Vertical helix	40	3	25
Spiral	100	2	32

3.1.1 GHE test system

To validate the results of numerical model for heat transfer simulation of the GHEs, temperature and volumetric flow rate data have acquired for different types of shallow GHEs in GSHP laboratory at ITU.

In the test system (Figure 3.4), flow rate, inlet and outlet temperatures are measured and recorded in real-time for each pipe by PT1000 temperature sensors and liquid turbine flow-meter. Before the test system is operated, temperature sensors are calibrated in a calorimetric container to get the same results from each sensor for the

temperature range of from 2 °C and 55 °C. Flow-meters are also calibrated by Siemens Mag5000 flow-meter.

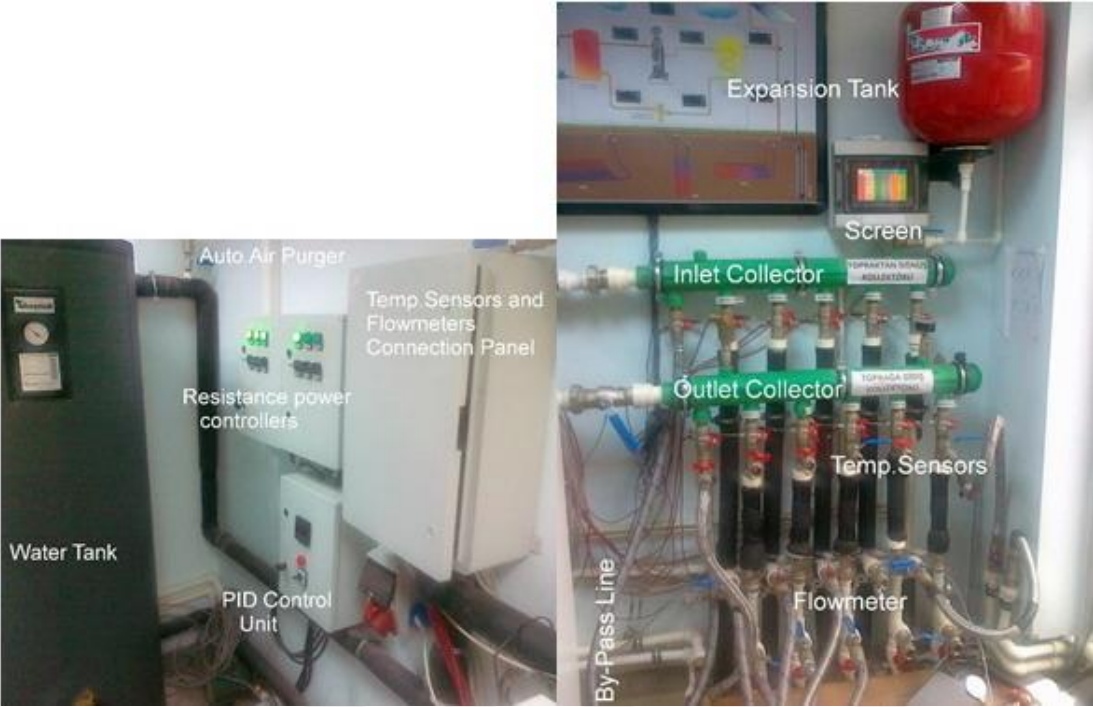


Figure 3.4: Experimental Test System

To test the pipes connected to the test system. After the air purged from the system, undisturbed ground temperature has to be measured before the test is started. To determine undisturbed ground temperature the valves 3, 5, 6, 7 are closed (in Figure 3.5) and running the pump, circulating water temperature after 15-20 minutes gives the information about the undisturbed temperature.

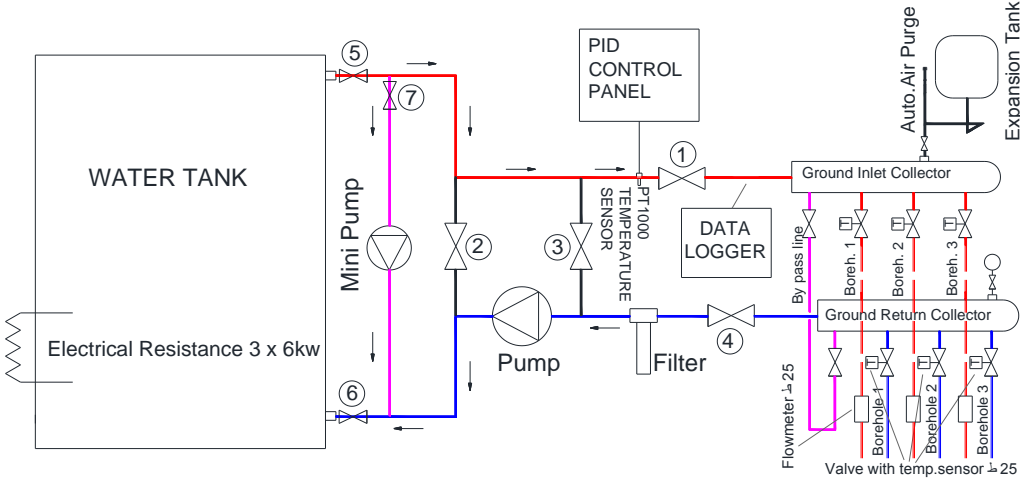


Figure 3.5: Constant Temperature TRT System

Later than, valves 2, 3, 7 and borehole's valves are closed, mini pump and electrical resistances with PID control are run to heat the water in the tank up to test temperature. When the tank temperature achieved to the test temperature, by-pass line and valves 2 and 3 are closed, valve 7 is half opened and the others are fully opened, and then test is started. Mini pump on the tank provide homogeneity of tank temperature. Inlet temperature is measured and controlled by PID controller.

3.1.2 Heat pump test system and and example for COP measurement

In order to evaluate the COP value of a heat pump, we need to keep some temperatures constant. For instance, the temperature of the fluid in exit and entrance of condenser should maintain at 45 and 40 °C and also in evaporator exit and entrance should keep at 7 and 10 °C. For preparing these conditions we placed two tanks contained of water, one of them represents ground and the other one the building. Figure 3.6 demonstrates connection interface of COP test system in the lab.

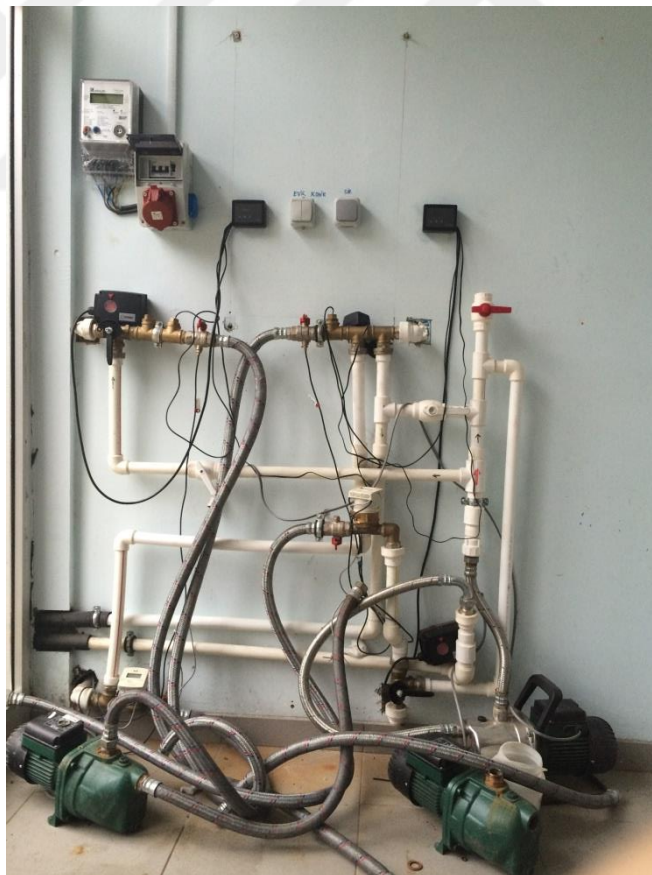


Figure 3.6: Connection interface of heat pump COP test system

After applying the mentioned conditions in last part to heat pump system, COP value of a definite GSHP system is measured. Table 3.3 shows experimental results for 24 hours non-stop operation. Furthermore, COP of the system can be measured by simple equation 3.1. Different measured parameters are given in Table 3.3.

The model of GSHP system is SensoTherm BSW designed by BRÖTJE. The COP value of the tested heat pump under the conditions that were discussed in Part 3.3 is given as 4.2 nominally. Figure 3.7 shows that the averaged COP value of the system is approximately equal to 4.2. Oscillations results from the oscillations of controlled temperatures due to low precise control.

Table 3.3: Heat pump COP test results.

Time	W [kWh]	Q _H [kWh]	Q _C [kWh]	COP _{HP}	COP _R
9 AM	22.384	233.6	19.9	-	-
1 PM	23.575	238.7	23.8	4.281	3.300
5 PM	24.407	241.9	26.2	4.103	3.101
9 PM	25.06	244.7	28.3	4.288	3.216
1 AM	25.734	247.7	30.7	4.45	3.540
5 AM	26.689	251.7	33.7	4.188	3.204
9 AM	27.961	257.1	37.8	4.128	3.223

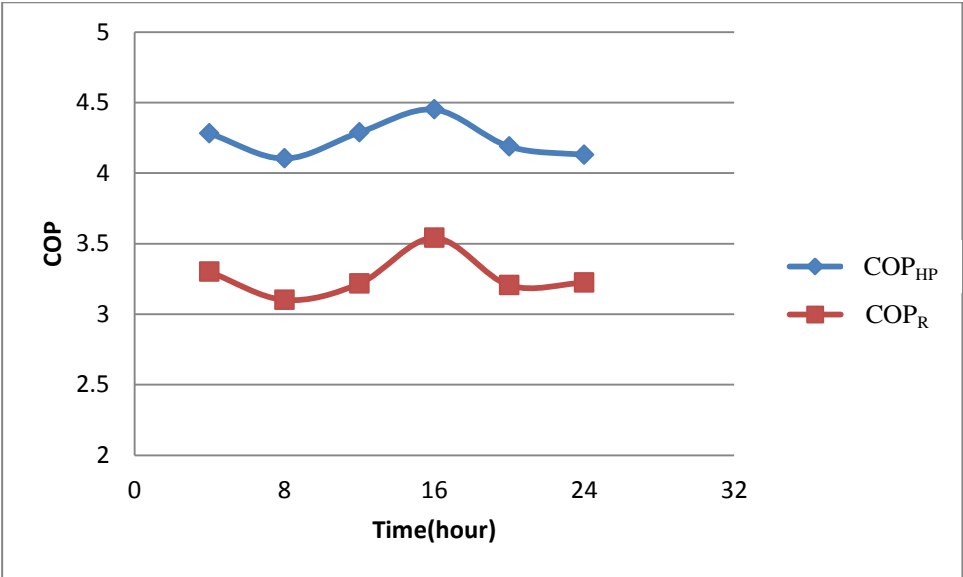


Figure 3.7: COP cooling and heating test results

3.2 Shallow GHE Test Results

In this part the results of HTR in different shallow GHEs are described. Shallow GHEs are snail, slinky and helix. helix has different properties than other GHEs. To compare all GHEs, in the first step snail, slinky types are compared. In the testing process each GHE system tested for 70 hours sending specific constant temperature fluid to the GHE. Testing fluid temperature is chosen as 40 °C to simulate summer conditions for non-stop working. To get reliable results all tests are done twice in different times. To avoid effecting of ground previous tests at least two weeks waited between the tests. Figure 3.8 shows test results of snail, vertical and horizontal slinky types. variation of heat transfer rates from start to end of the test can be seen in this figure. Vertical slinky started higher HTR and then after period of time (about 12hours) decreasing of HTR become linear. Horizontal slinky shows similar behavior to the vertical slinky but snail type shows different behavior than them. It is almost linear decreased all the test period (Aydin et al, 2015).

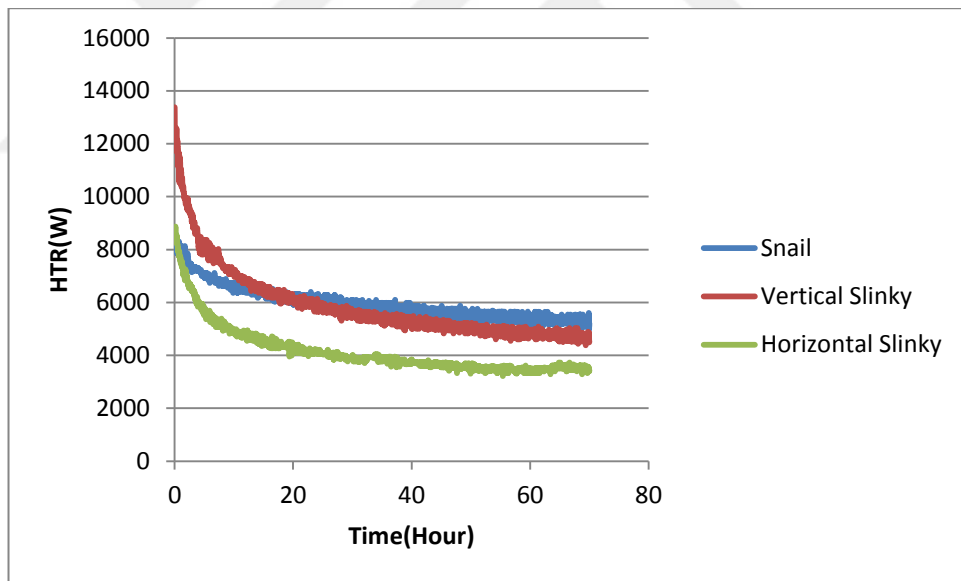


Figure 3.8: Shallow GHE test results (Aydin et al, 2015).

3.3 Helix GHE Test Conditions and Results

In this part the results of vertical and horizontal helix GHEs are given. In order to better understand the behavior of the system, the performance of GHEs during 5 days is experimentally analyzed. Figure 3.9 shows the evolution of the inlet and outlet temperatures in the indoor and outdoor circuits in vertical helix GHE. As shown in

Figure 3.9 inlet water temperature is almost in constant value of 40 °C. The ground return temperature reaches the maximum value of 39.2 °C. It can also be observed that the outlet water temperature from the ground approaches a higher and constant value for longer duration due to increment of ground temperature. Based on this temperature evaluation, we consider that the temperature of the pipes wall is almost constant and is equal to the average value of inlet and outlet temperatures.

Characteristics of different helix GHE parameters are shown in Table 3.4 and Table 3.5.

Table 3.4: Characteristics of the helical-shape GHE pipes

Parameters	
r_o [mm]	12.5
r_i [mm]	10.5
L_p [mm]	80
D [mm]	400
n	36
L_{GHE} [mm]	3000
K_{PE} [W m ⁻¹ K ⁻¹]	0.38
C_{PE} [j Kg ⁻¹ K ⁻¹]	1900
ρ_{PE} [Kg m ⁻¹]	958

Table 3.5: Characteristics of ground and working conditions

Parameters	
C_p [j Kg ⁻¹ K ⁻¹]	850
k_{eff} [W m ⁻¹ K ⁻¹]	3.5
ρ [Kg m ⁻¹]	2160
T_{avg} [°C]	39.6
T_e [°C]	16.5
T_{avg-i} [°C]	40.0
T_{avg-o} [°C]	39.2

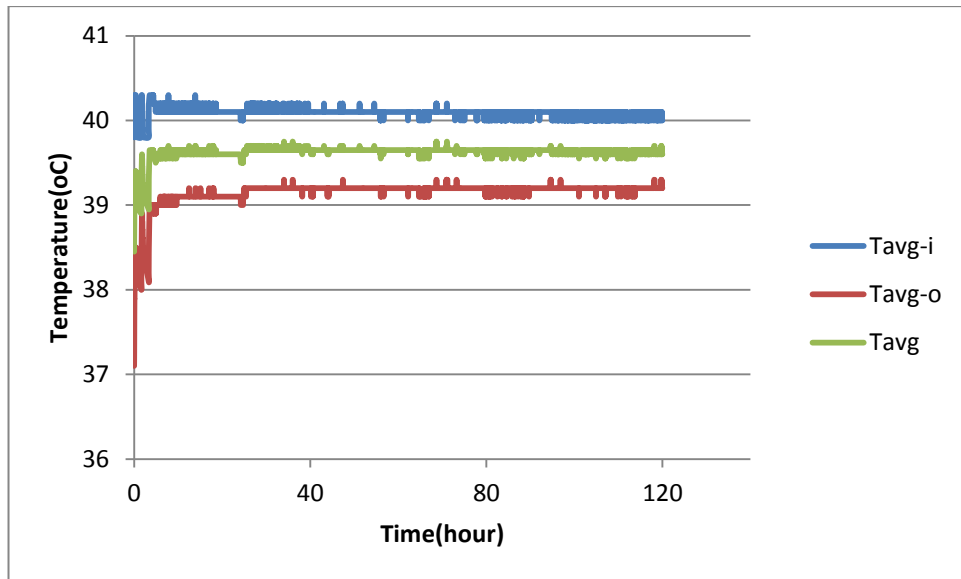


Figure 3.9: Inlet and outlet water temperature evaluation in 120 hours operation.

Figure 3.10 shows the HTR of single vertical and horizontal helix GHE for 120 hours operation. As it is obvious from the Figure 3.10, performance of the GHE decreases by the time and also HTR of horizontal helix is less than vertical one. HTR is directly affected by the temperature of soil and GHE wall. GHE was tested in September 2013. During 2013 the temperature of the ground in different depths was measured by using 15 sensors located in different depths of the ground. Figure 3.11 illustrates temperature of ground that were collected in ITU GSHP laboratory. The reason of difference between vertical and horizontal HTR values is the difference in ground temperature. Horizontal GHE is placed in -1.5 m and the average ground temperature is 22 °C in this zone. Vertical one is located between -1.5 and -4.5 m, the average ground temperature here is 16.5 °C.

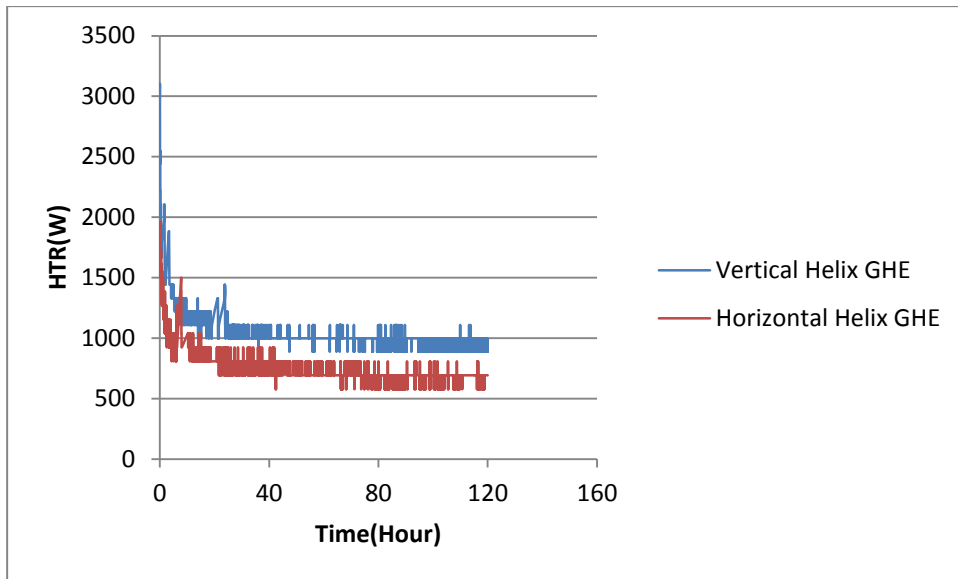


Figure 3.10: HTR of helix GHE for 120 hours non-stop operation.

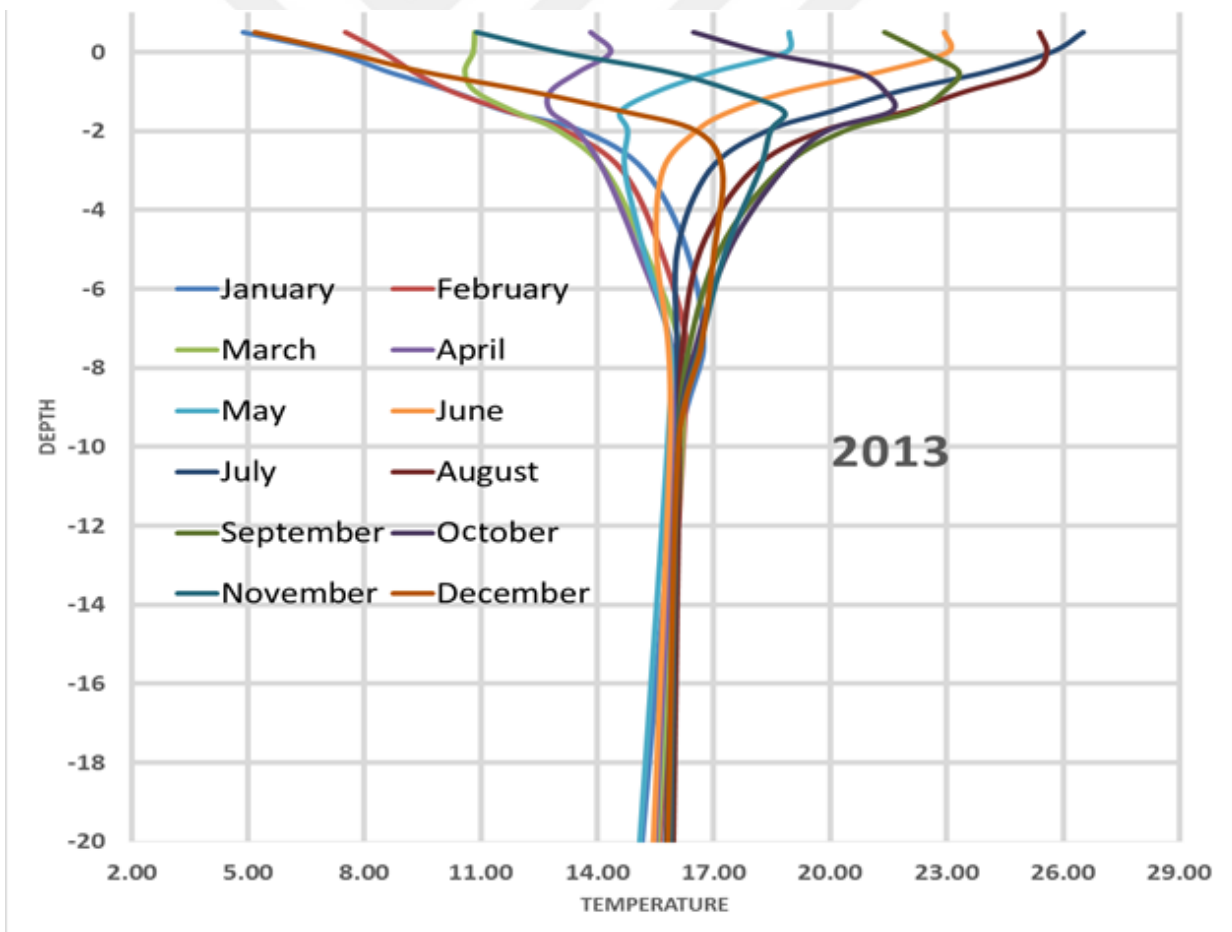


Figure 3.11: Ground temperature variation at ITU Energy Institute fie

4. SIMULATION

4.1 Modeling Purpose

In recent years, GSHP systems have been widely applied in residential and commercial buildings. Due to the superiority of high energy-efficiency, environmental friendliness and low maintenance GSHP systems have attracted more and more attention. The major costs of vertical GSHP systems depend on the length, diameter and numbers of GHEs. Analysis on heat transfer in subsurface is important to size the GHE that optimum performance is achieved with minimum costs.

To reduce the high cost of experimental setups for different configuration of helix GHE, computational 3D models are constructed for different configurations.

4.2 Model Description

To evaluate HTR value of the GHEs, a numerical model is developed in COMSOL environment. In COMSOL, GHE can be modeled by fully discretized meshes. This program has been practically proved to be a suitable way for simulating HTR values of GHE. In order to analyze helix GHE, 3D models are developed. The model cases are shown in Figure 4.1, 4.2 and 4.3

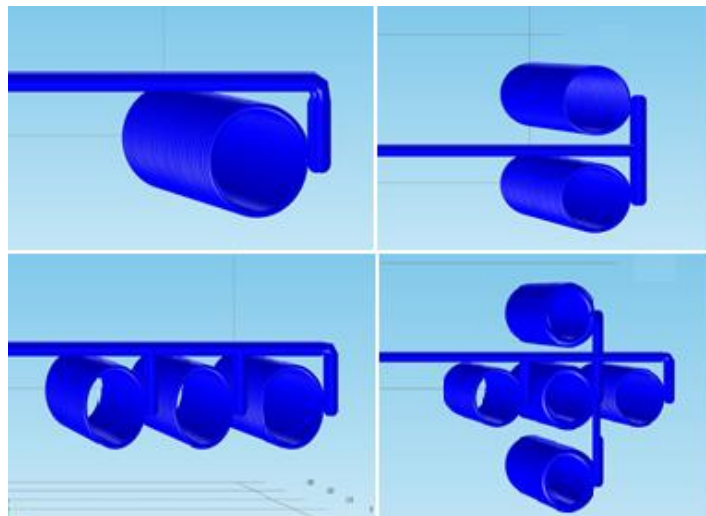


Figure 4.1: Different configurations of vertical helix GHEs

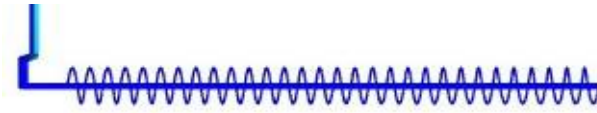


Figure 4.2: Horizontal helix GHE COMSOL model

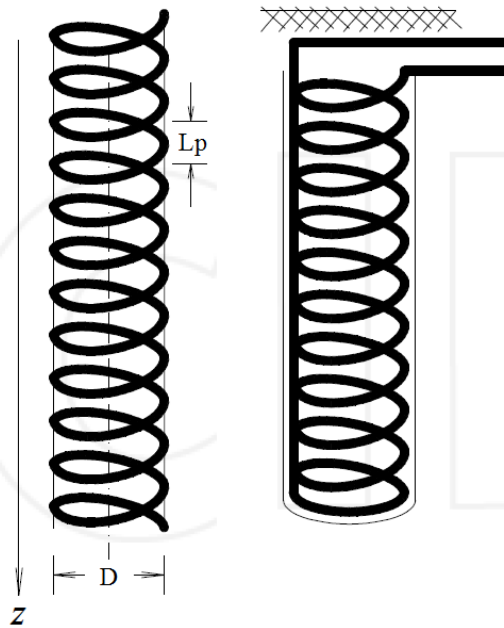


Figure 4.3: Schematic view of helix GHE.

The heat transfer from the pipe wall of the GHE to the ground depends on the turns number, location, material and configuration of the pipes. For modeling the heat transfer of a GHE, the ground soil/rock is usually approximated as an infinite homogeneous medium and heat transfer is assumed mainly taking place by conduction. The wall temperature of GHE is assumed as constant and is equal to average value of inlet and outlet water temperature. Also different characteristics of soil in the ground such as thermal conductivity and specific heat capacity play an important role in GHE performance. The other crucial factors that directly affect the GHE performance is the temperature of the soil layers.

The temperature of the ground is a function of the soil thermal properties (Bose et al, 1985): thermal diffusivity ($\alpha = k/\rho c_p$), thermal conductivity (k) and the heat capacity (C_p). The soil thermal diffusivity is a defined property and is the ratio of the thermal conductivity and the heat capacity. Therefore, three soil properties k , α and C_p should be known or estimated to predict the thermal behavior of GHEs. These

parameters are commonly assessed via laboratory measurements or field tests. In laboratory, thermal conductivity is generally measured using the specimens gathered from the borehole field. Drilling cores are often collected during the drilling works and used for the preparation of specimens. Obtaining accurate values of the thermal properties of the soil requires a detailed site survey. Soil composition varies widely not only with locations but also from wet clay to sandy soil.

Following assumptions are made in all models:

- a) Ground is an isotropic and homogeneous medium and also may contain some water in some layer of it. Therefore because of these water possibility in the soil, the effective thermal conductivity can be higher than the thermal conductivity of the soil itself.
- b) The temperature change along the vertical direction is negligible.
- c) The fluid temperature in the GHEs is assumed equal to the average of inlet and outlet temperatures.

4.3 Single Helix GHEs Computational Results and Validations

The accuracy of the simulation is verified by comparing the results of simulation with the experimental one. In this part of the study, only one GHE is considered. The average inlet temperature and the flow rate of the experiment are taken as 39.59 °C and 15.9 l/min. Experimental results are obtained for 120 hours non-stop operation and the results of computational model are based on aforementioned assumptions.

Figure 4.4 shows the experimental and computational results for the variation of HTR values of horizontal and vertical helix GHEs with time. This HTR values (performance) decrease due to heat transfer between GHE and ground.

As it is shown in Figure 4.4, experimental and computational results are in good agreement which proves the accuracy of our model.

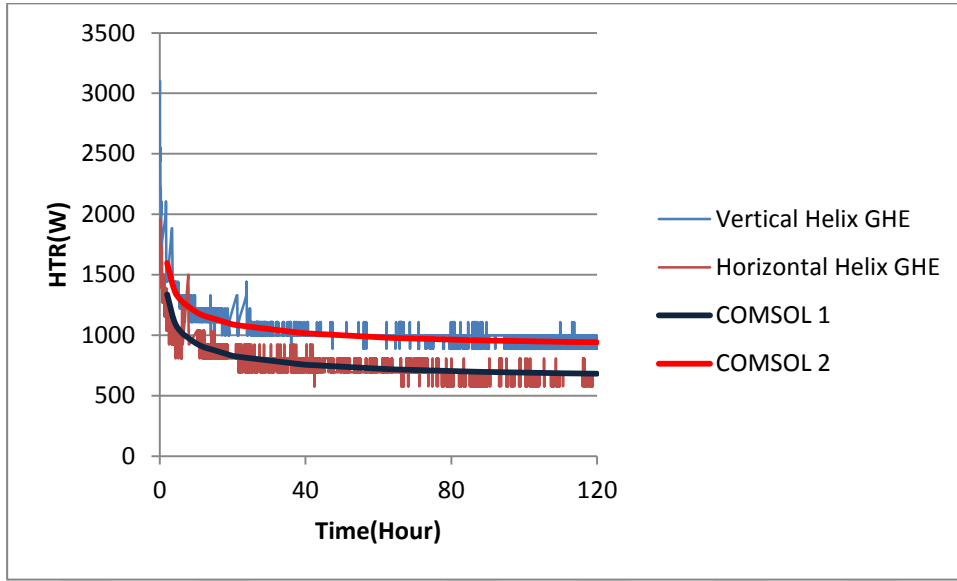


Figure 4.4: Single horizontal and vertical helix GHE model validation for 120 hours non-stop operation experiment.

It is noted that in these modeling, COMSOL solves time dependent conductive heat transfer equation given below:

$$\rho c_p \frac{\partial T}{\partial t} = k_{\text{eff}} \left[\frac{\partial^2}{\partial z^2} + \frac{1}{r} \frac{\partial}{\partial r} \left(r \frac{\partial}{\partial r} \right) \right] \quad (4.1)$$

Initial and boundary conditions for equation 4.1 are as follows:

$$T(0, r, z) = 16.5 \text{ } ^\circ\text{C} \quad (4.2)$$

$$T(t, \infty, \infty) = 16.5 \text{ } ^\circ\text{C} \quad (4.3)$$

$$T(t, r_H, z_H) = 39.6 \text{ } ^\circ\text{C} \quad (4.4)$$

The main purpose of this study is to analyze the vertical helix GHEs since it has higher HTR value. Therefore, all results given in following parts are related to vertical helix GHEs.

Figure 4.5 and Figure 4.6 describe the variation of temperature distribution around vertical helix GHE with time. As it is shown in Figure 4.6, numerical results state that average soil temperature increases with time. Furthermore, this graph helps us in placing the other GHE near a single one, the distance between them can

approximately be estimated. More information about more than one helix GHE is investigated in the second part.

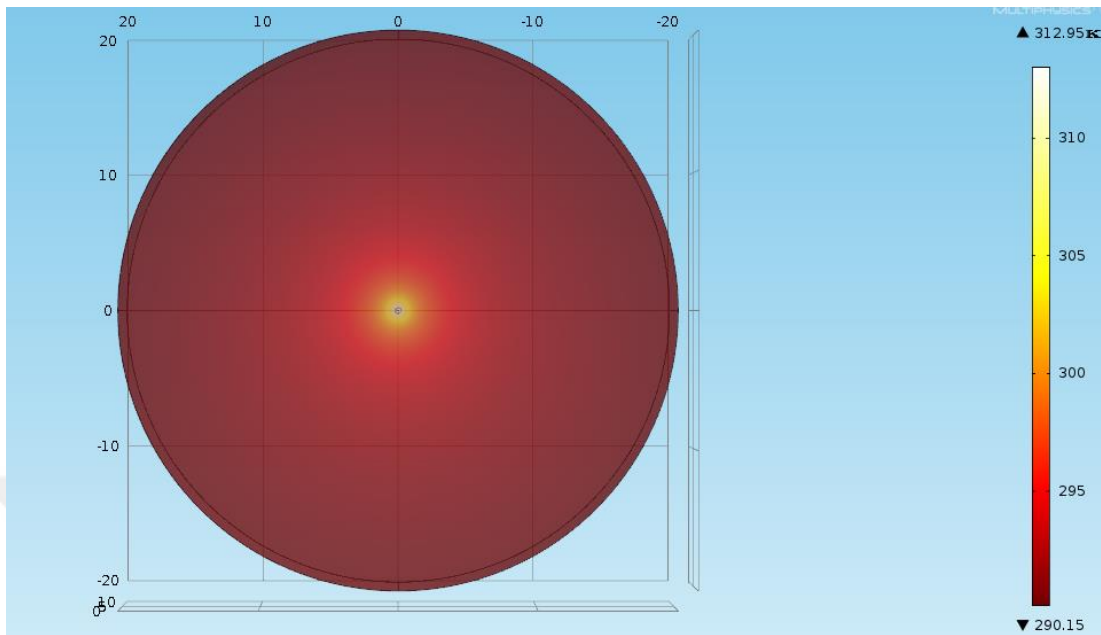


Figure 4.5: Numerical temperature distribution in the ground at the end of 3 months operation around single vertical helix GHE

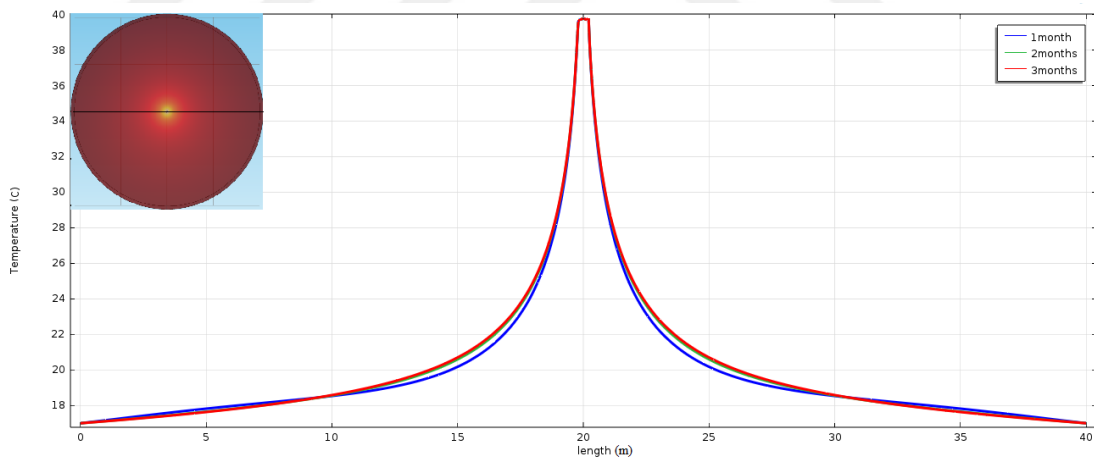


Figure 4.6: Temperature distribution around single helix GHE at the end of one, two and three months.

4.4 Computational Results for Multi Vertical Helix GHE and Examination of Performance Loss

4.4.1 Prediction of performance losses

By comparing the single GHE HTR value with those of 2, 3 and 5 GHEs, performance losses can be determined by the following expression:

$$\text{Performance Loss} = 1 - \frac{\dot{Q}_{cGHE}}{\dot{Q}_{sGHE}} \quad (4.5)$$

Performance losses occur because of thermal interaction between GHEs. The HTR value of critical GHE is determined in each GHEs configuration computationally and performance losses are calculated for different distances between GHEs, which varies from 1 m to 11 m. The critical GHE is defined as the central GHE in all configurations.

Figure 4.7 indicates the performance losses in different configurations of GHEs. Based on the designer's objective, optimum distances between GHEs can vary. Thus, analysis of performances and costs of different configurations has been a task for investors and engineers.

As it is seen from Figure 4.7, when the number of GHEs is increased in a finite size domain, increment of the system performance becomes smaller for addition of each GHE. It is found that when the distance between GHEs is $d=3\text{m}$, performance losses of critical GHE (cGHE) for the cases of 2, 3 and 5 GHEs are around 6%, 14% and 22% respectively. Similarly when the distance is 10m, performance loss is 1%, 2% and 4% for 2, 3 and 5 number of GHEs.

In engineering problems generally the performance losses less than 5% is acceptable (Ozisik, 1993). As it is illustrated in Figure 4.7, the performance losses are less than 5% if distance is more than 5 m, 7 m and 9 m for two, three and five GHEs configuration respectively. On the other hand, this value depends on the investors and engineers who consider financial and technical performance criteria.

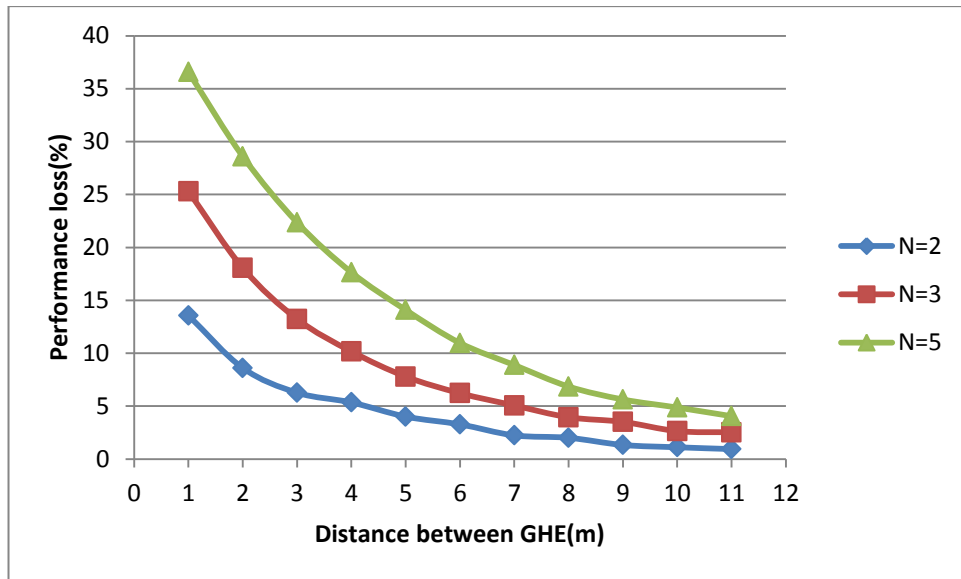
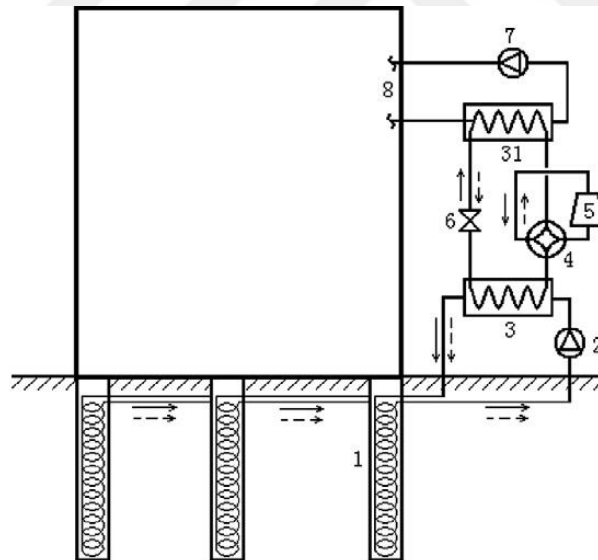


Figure 4.7: Performance losses of critical GHE at the end of 3 months non-stop operation.

In order to better understand the placing of vertical helix GHEs, the schematic view of three GHEs integrated with heat pump is demonstrated in Figure 4.8.



- (1. PGHE; 2,7. circulation pump; 3,31. condenser and evaporator;
- (2. 4. reversing valve; 5. compressor; 6. expansion valve;
- (3. 8. conditioned space)

Figure 4.8: Schematic diagram of a GSHP system with three helix GHEs (Cui et al, 2011).

By taking all above mentioned arguments into the consideration, it is obvious that optimum distance should be chosen from Figure 4.9. We choose 7 meters distance between GHEs, because in that case performance loss is less than 10% and this choice gives much more economical application opportunity. In this figure, variations of performance losses of vertical helix GHEs with time are shown for different configurations. Performance loss increase with time and the number of GHEs.

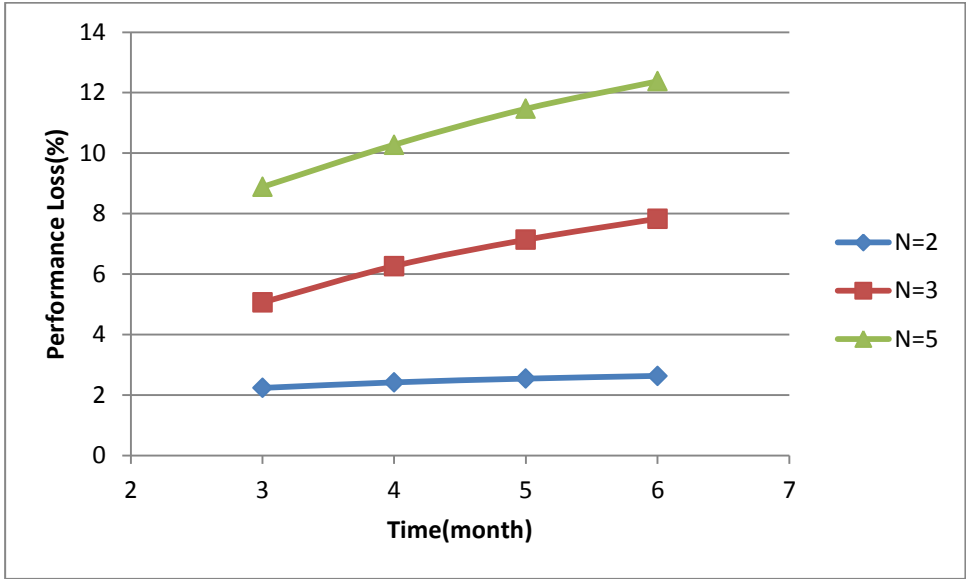


Figure 4.9: Time dependency of performance losses in case of 7 meter distance between GHEs

4.4.2 Determination of temperature distribution around GHEs

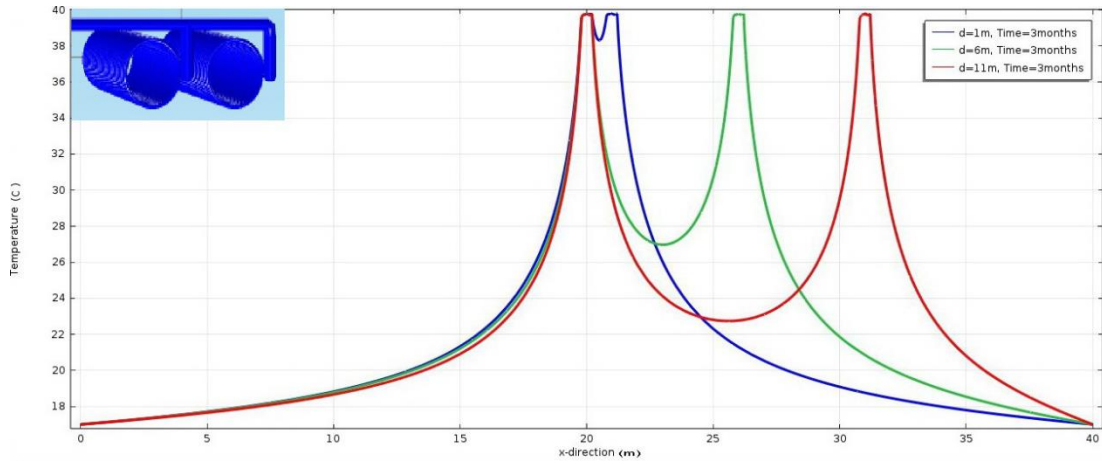
Figure 4.10 shows the ground temperature profiles at various distances from the GHE after 3 months non-stop operation. The temperature profiles in the ground are affected by GHEs configuration.

The comparison of temperature profiles at the end of 3 months non-stop operation and $z=1.5$ m, with different distance between GHEs is shown in Figure 4.10 for different configurations. A comparison for different time values in case of constant distance between GHEs is presented in Figure 4.11.

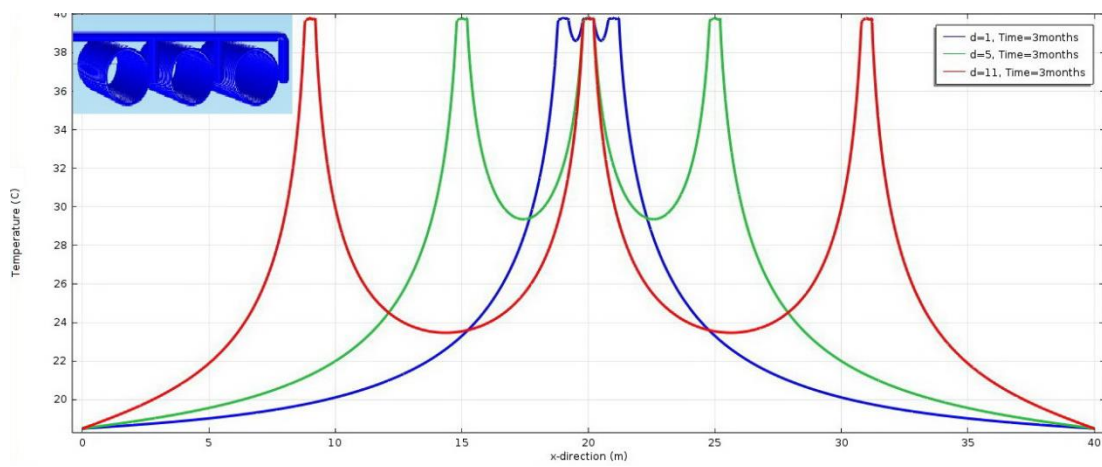
According to the comparisons shown in Figure 4.10 and Figure 4.11, the temperature profiles in the ground are highly affected by GHEs configuration. It can be seen that

an apex of the temperature distribution appears at the circumference of each GHE. It is obvious from these figures that the ground temperature is raised by the time and temperature response at any location keep rising and also for a specific distance from each borehole, the temperature of the region between the boreholes is higher than the temperature of the outer area. As it is shown in Figure 4.10a after running the system for 3 month the temperature of the soil at the central axis of two GHEs increases about 3°C, 7 °C and 19 °C when $d=11\text{m}$, $d=6\text{m}$ and $d=1\text{m}$ respectively. By increasing the number of GHEs, temperature distribution is also changed. As it is shown in Figure 4.11b the temperature of the soil increases about 3.5 °C, 9.5 °C and 19.5 °C when $d=11\text{ m}$, $d=5\text{ m}$ and $d=1\text{ m}$ at the middle point between two GHEs.

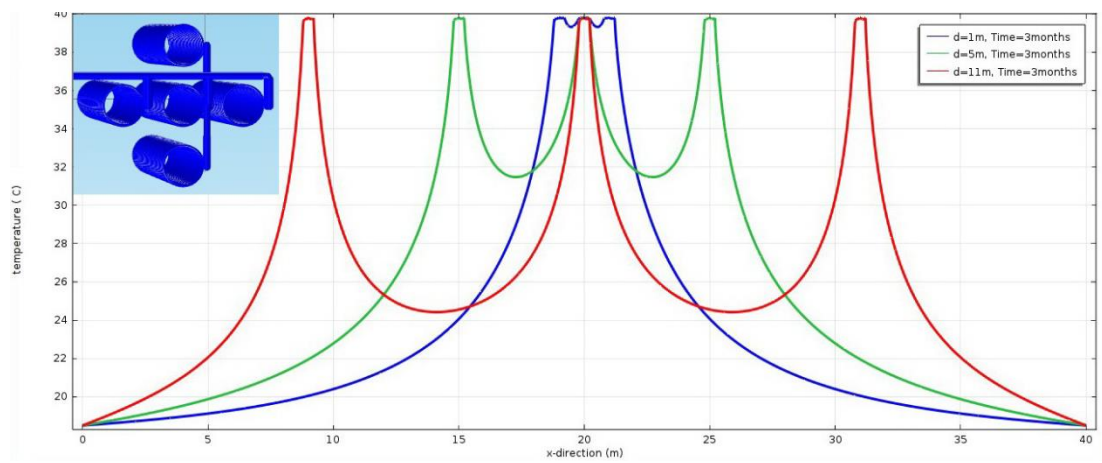
Figure 4.12 shows the schematic view of thermal interaction between GHEs. As it is seen, the thermal interaction between GHEs becomes higher when the number of GHEs increases and also distance between them decreases.



(a)

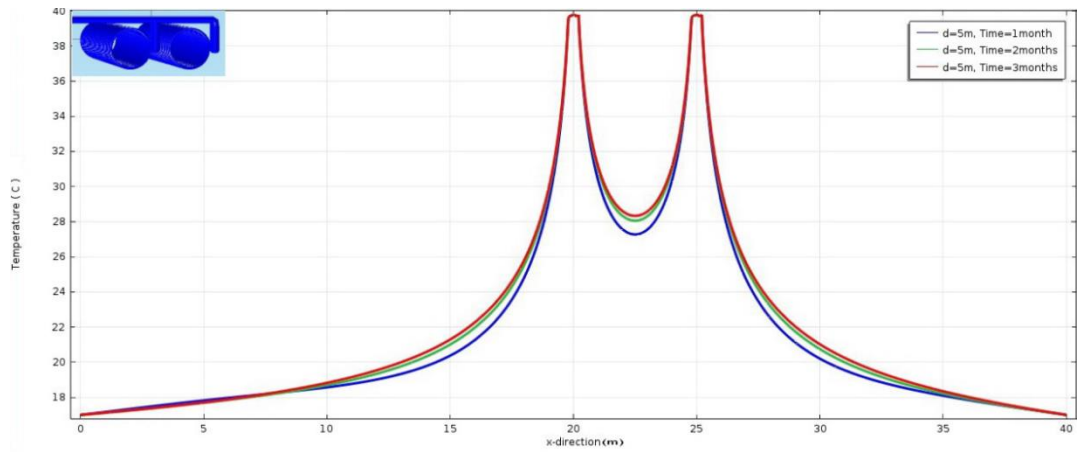


(b)

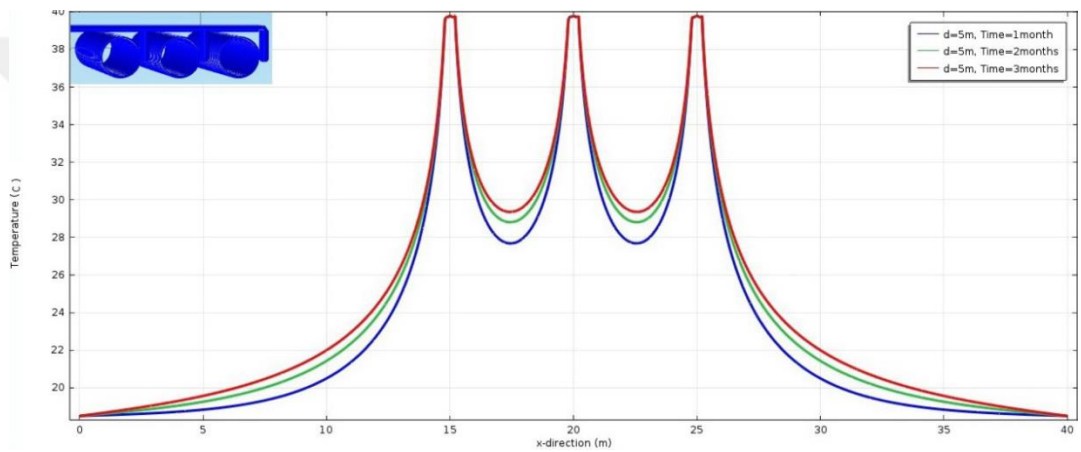


(c)

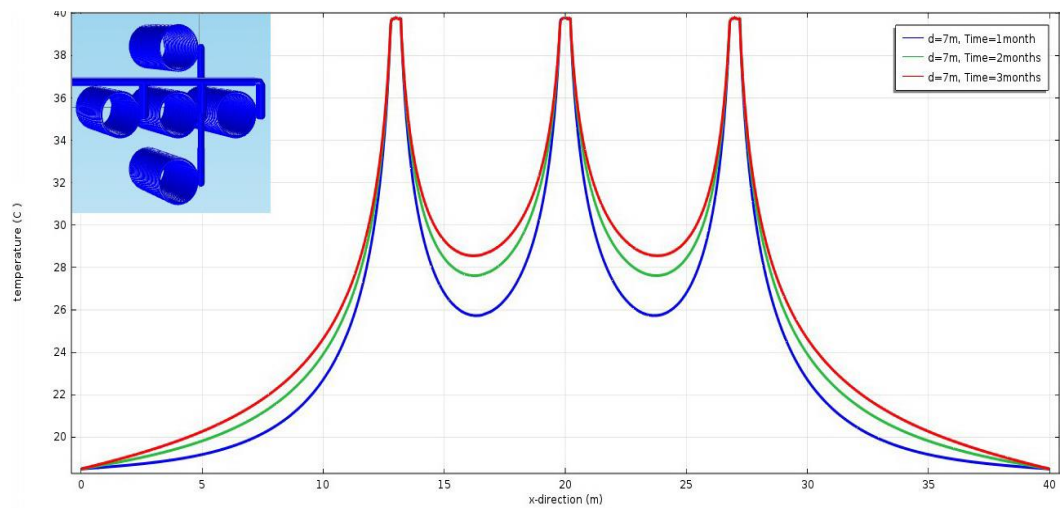
Figure 4.10: Effect of distances between GHEs in temperature distribution at $z=1.5\text{m}$ and at the end of 3months non-stop operation for (a) $N=2$ (b) $N=3$ (c) $N=5$



(a) $N=2$, $d=5m$



(b) $N=3$, $d=5m$



(c) $N=5$, $d=7m$

Figure 4.11: Temperature distribution in the ground at the end of 1, 2, 3 months non-stop operation for (a) $N=2$ (b) $N=3$ (c) $N=5$

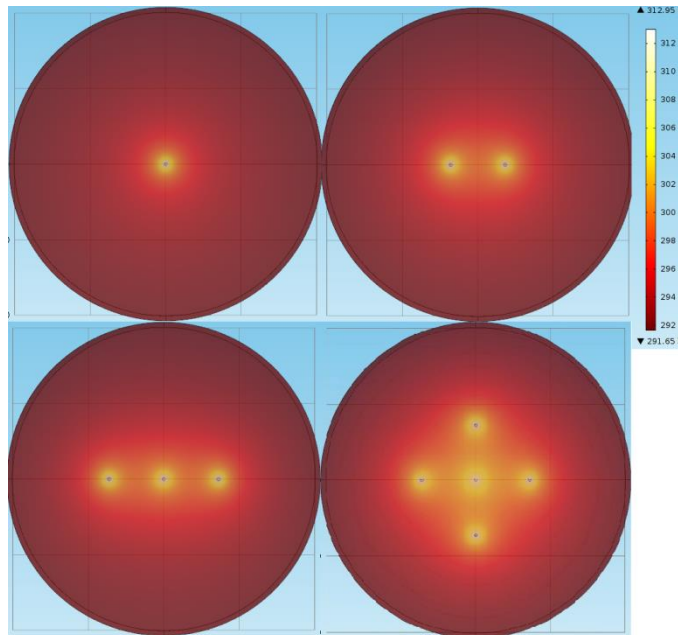


Figure 4.12: Schematic top view of temperature distribution in the ground at the end of 3 month non-stop operation with $d=7$ m

4.5 The Influences of the Pitch Distance (L_p) and Major Diameter (D) of a Single Vertical Helix GHE on it's HTR Value.

The pitch between the turns of the helix and GHE major radius play a crucial role in the design process. These parameters are geometric parameters that directly affect the HTR and initial cost of the installation for the system. These properties are directly related to the vertical lengths required to construct the heat exchanger as well as amount of excavation. The numerical simulations of a single vertical GHE are made for different L_p and D values. The effects of pitch distance and major diameter of helix GHE on its HTR value are examined (Figures 4.13 and 4.14).

To investigate the effects of L_p on HTR value of GHE, total length of vertical helix GHE is assumed as constant value. In this thesis total length of vertical helix GHE is 100 m. It is also equal to the amount of total length of used pipes.

Figure 4.13 and Figure 4.14 show the HTR of GHE for different values of L_p and D . It is seen that by increasing the L_p and D , HTR value of a GHE is improved. On the other hand, the total cost of embedding the GHE into ground becomes higher and higher by increasing the values of L_p and D . Therefore, it is important for designers and investors that they know the exact requirements of consumers.

The improvement of HTR value with longer and bigger exchangers results in increment of installation costs, which are the main drawback of GSHPs. During the designing of GHE fields, maximum heat load of the consumer is considered, and the minimum required borehole sizes (L_p and D) are chosen. On the other hand, trying to minimize the installation cost by decreasing the sizes of L_p and D alone, causes higher number of GHE which also increases the initial cost. Therefore, initial cost should be minimized by considering the whole system. Furthermore, not only the initial cost but also the operational costs should be considered during the optimization of the system overall costs. This requires the long term predictions of HTR value of a GHE.

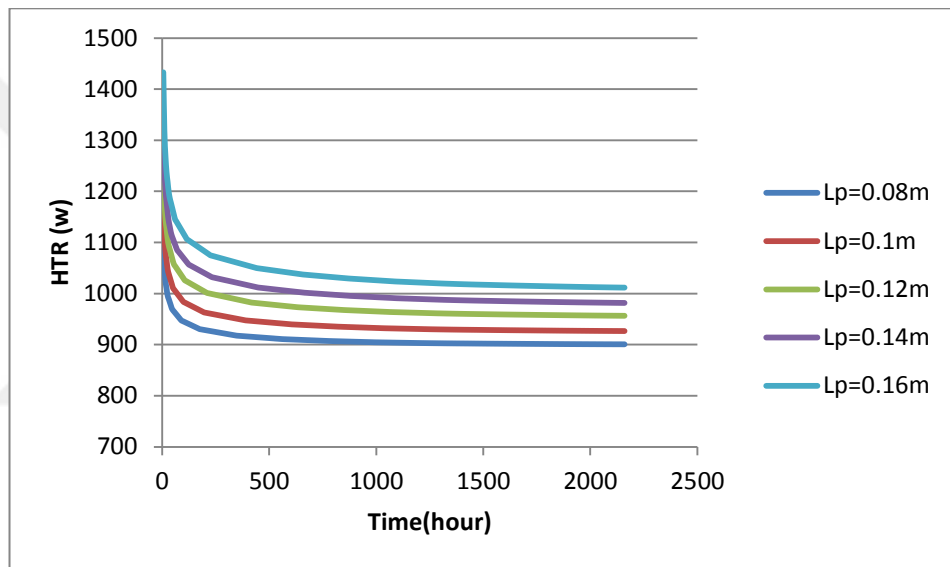


Figure 4.13: Effect of pitch (L_p) on HTR for 3 months non-stop operation

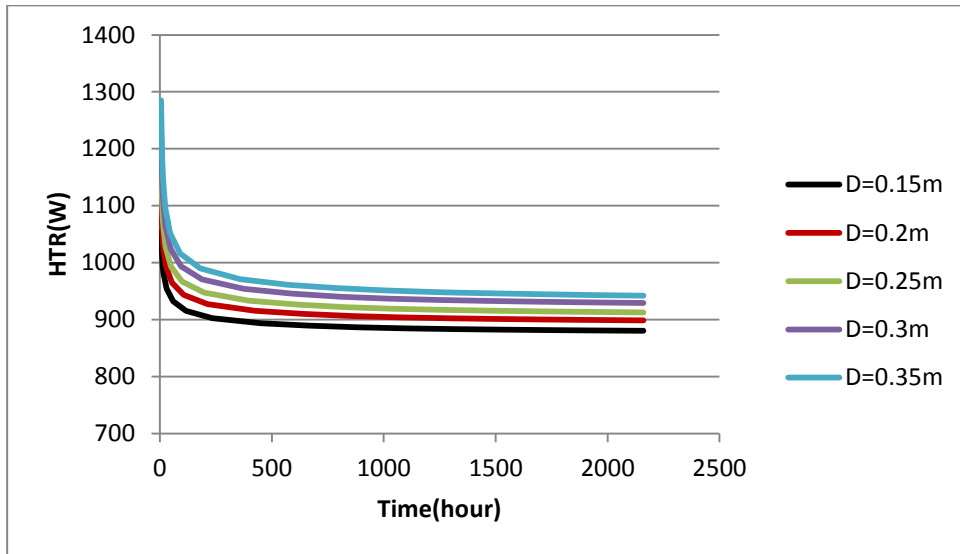


Figure 4.14: Effect of GHE major radius (D) on HTR for three months non-stop operation

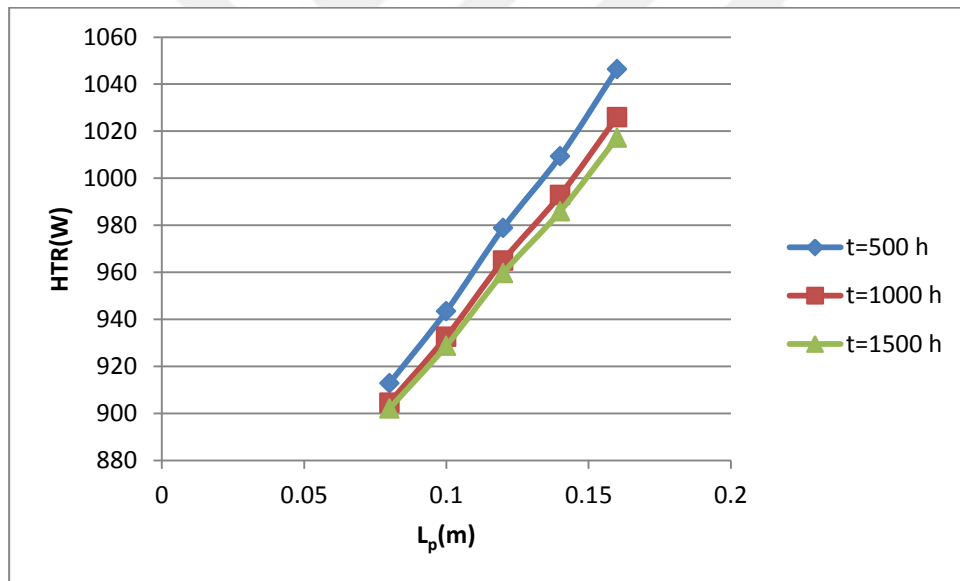


Figure 4.15: HTR value of a single helix GHE versus L_p for different operation times

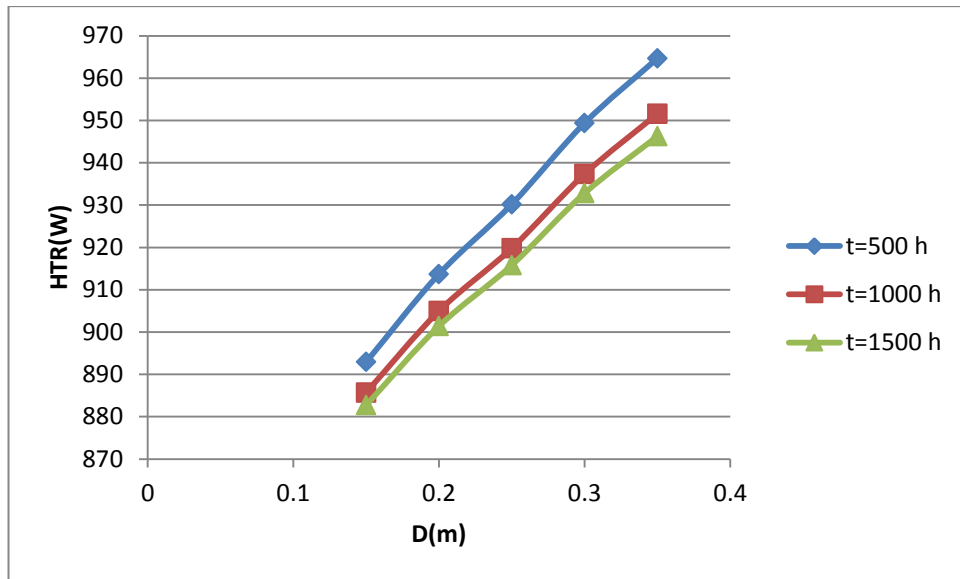


Figure 4.16: HTR of a single helix GHE versus D for different operation times

Variations of HTR value with L_p and D are seen in Figures 4.15 and 4.16 respectively. These figures show that the average HTR values linearly increase with the value of D and L_p . These linear dependencies are due to the increment of peripheral surface area and heat capacity of ground per turn. Since the time variation of HTR value decreases with increasing time, lines given in Figures 4.15 and 4.16 are getting closer to each other for longer operation times.

4.6 A Typical Example for Vertical Helix GHE Analysis

In this part, a building with 120 m^2 heating/cooling area is considered. For heating and cooling of this building, GSHP system with vertical helix GHE is chosen. Schematic view of building is shown in Figure 4.17. As it is stated in different references, general required heat load in Turkey for a standard building is approximately 80 W/m^2 . Therefore total heat load of this building is 9600 W . Furthermore, COP value of a heat pump is assumed as 4.0. In this case, 7200 W heat is needed to pump from ground to building.

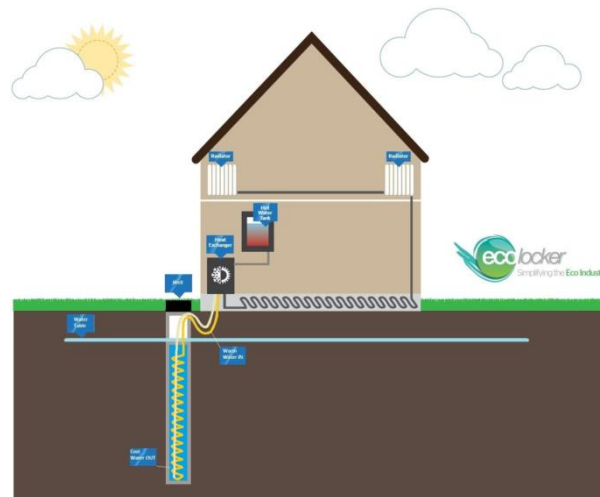


Figure 4.17: Building with vertical helix GHE

To predict the number of GHEs that are needed for heating and cooling applications, first of all long term performance of a single vertical helix GHE should be estimated. Again by using COMSOL and based on previous validated data, HTR value of a single vertical helix GHE is numerically predicted. The averaged HTR value is around 870 W for 1-6 months time interval.

In GHE designing procedure generally the most critical conditions are considered. The system is assumed to work 6 months non-stop in heating or cooling mode. For 6 month operation, COMSOL results show that averaged HTR of a single vertical helix GHE is 870 W. By taking all the above arguments into consideration it is concluded that 9 vertical helix GHE is needed for this building. For more than 5 GHEs, we assume that five GHEs graph can be used for performance loss prediction with an acceptable error. By looking at Figure 4.7, ten meter distances between GHEs are chosen. For this distance, performance loss is less than 5%. Based on consumers utilization and designers goals this amount can of course be vary. The suggested configuration is shown in Figure 4.18 for most critical conditions (6 months non-stop operation). In this configuration, performance loss is predicted less than 5%.

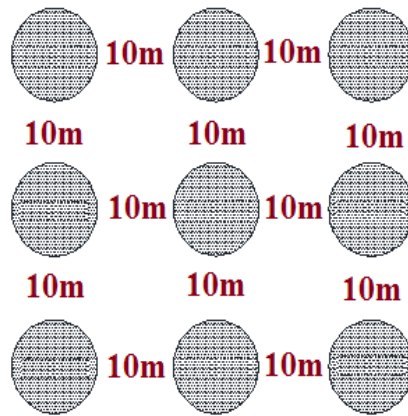


Figure 4.18: Nine vertical helix configuration

To confirm our modeling for nine GHEs, COMSOL model is also run for this configuration. Numerical analysis shows that performance loss is 6.68%. Numerical results are also confirming the accuracy of our designing with an acceptable error. Figure 4.20 shows the thermal interaction between GHEs at the end of 6 months non-stop operation.

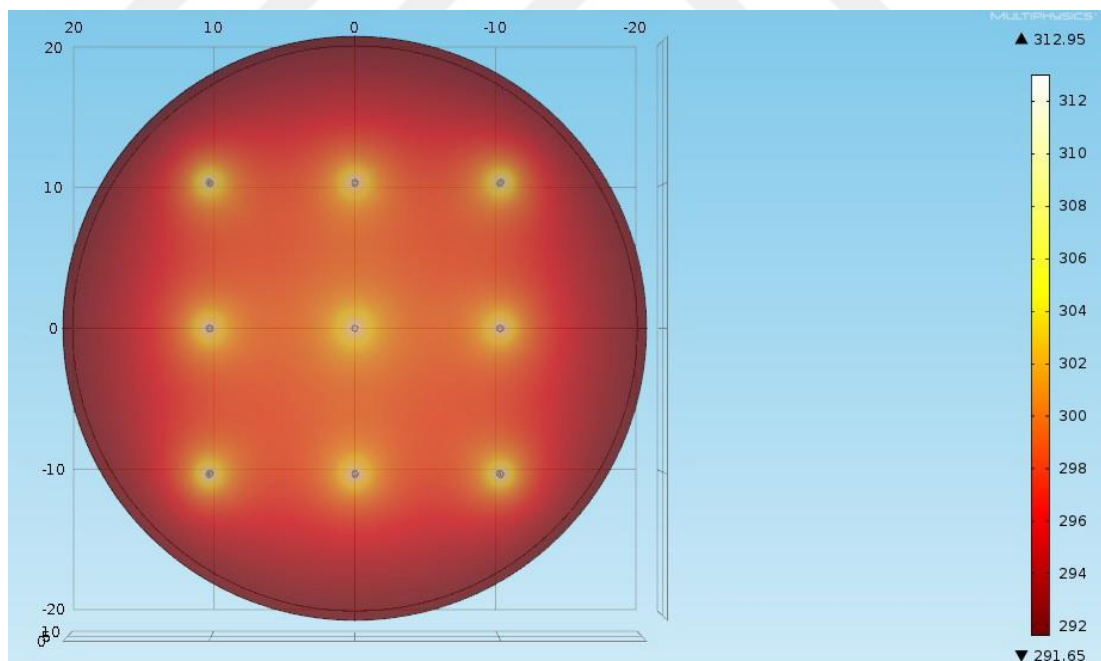


Figure 4.19: Thermal interaction between nine vertical helix GHEs for 6 month non-stop operation

Sometimes the application area is limited and there is no enough space for placing GHEs. In that case, more performance losses can be accepted to minimize the application area. For nine vertical helix GHEs, the following configuration can also

be used. In corners and sides we can use three GHEs performance loss graph. In Figure 4.7 for three GHEs 8 meters distance is suitable. Figure 4.21 demonstrates other configuration of nine GHEs that can be used.

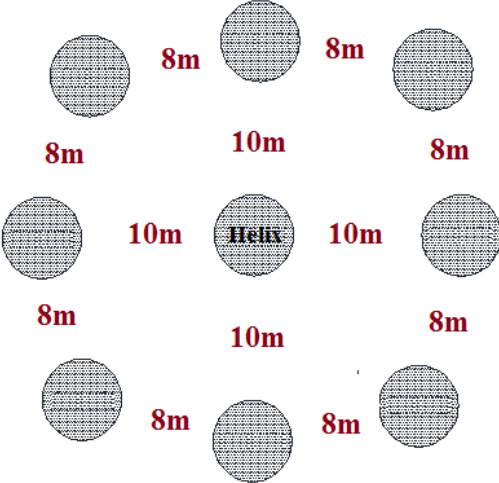


Figure 4.20: Other configuration type of nine vertical helix GHEs

5. CONCLUSIONS AND RECOMMENDATIONS

This thesis presents the analyses of different parameters on the performance of vertical helix GHE for GSHP systems. The most important parameters, which influence the performance of GSHPs, have been thoroughly analyzed, running long-term simulations and estimating the performance losses for each GHE configuration. In order to show the accuracy of our simulation, we compare the modeling results with available experimental data. As it is discussed, computational and experimental results are in good agreement.

The results of the simulations prove that L_p and D are one of the important parameters in the design of a GSHP. Although increasing these parameters can improve the efficiency of GSHP, a larger investment is needed for installation. Therefore an optimum length should be found, which minimizes the total cost over the plant lifetime for an acceptable performance value.

In the large number of GHE, one of the most essential parameters that affect the system performance is distance between GHEs. In this study, the optimization process is performed separately for each number of GHE to estimate the range of the optimal distances between GHEs and how the optimal distance vary from month to month and also for different number of GHEs. As it is shown in Figure 4.7 the performance losses are less than 5% if the distance between GHE is more than 5 m, 7 m and 9 m for 2, 3 and 5 GHEs configuration.

Also the model presented in this study has been used to examine the temperature distribution development of different GHEs configuration. The temperature distributions around GHEs are determined for different distances between GHEs. The model seems to be compatible for showing the temperature distribution development around GHEs with time.

The simulations given in this study represent some new results which have not been published yet in literature of GSHP technologies. This computational model may provide useful guidance for designing the helix GHE for GSHP systems.

Finally, the complete COMSOL model presented in this work can be used as a tool to develop control strategies in order to optimize the system energy performance and ensure users' comfort along the year.

In the future, the following studies can be done to extend the study given in this thesis:

- a) Green's function method for performance prediction of helix GHE in case of constant wall temperature
- b) Constant heat flux model for helix GHE
- c) Investigating the applicability of using helix GHEs in deeper layers and also analyze its performance as well as total costs.

REFERENCES

- Ascione, F., Bellia, L., Minichiello, F.** (2011). Earth-to-air heat exchangers for Italian climates, *Renewable Energy* 36 (2011) 2177-2188.
- Aydin M, Sisman A, Gultekin A, Dehghan B.** (2015). "Experimental and Computational Performance Comparison between Different Shallow Ground Heat Exchangers", *World Geothermal Congress April 2015, Australia-New Zealand*.
- Bakirci, K.** (2010). Evaluation of the performance of a ground-source heatpumpsystem with series GHE (ground heat exchanger) in the cold climate region. *Energy* 2010;35:3088–96.
- Banks D.** (2008). *An introduction to thermogeology: ground source heating and cooling*. Blackwell Publishing.
- Bose, J., Parker, J., McQuiston, F.** (1985). *Design/data manual for closed-loop ground coupled heat pump systems*. Atlanta: ASHRAE; 1985.
- Çengel, Y., Boles, M.A.** (2011). *Thermodynamics: An engineering approach*. 7th Edition, New York: McGraw-Hill.
- Congedo, P.M., Colangelo, G., Starace, G.** (2012). CFD simulations of horizontal ground heat exchangers: a comparison among different configurations, *Applied Thermal Engineering* 33e34 24e32.
- Cui, P., Li, Z., Manc, Y., Fang, Z.** (2011). Heat transfer analysis of pile geothermal heat exchangers with spiral coils. *Applied Energy* 88 (2011) 4113–4119.
- Esen, H., Inalli, M., Esen, Y.** (2009). Temperature distributions in boreholes of a vertical ground-coupled heat pump system, *Renewable Energy* 34 (2009) 2672–2679.
- Fan, R., Jiang, Y., Yao, Y., Ma, Z.** (2008). Theoretical study on the performance of an integrated ground-source heat pump system in a whole year. *Energy* 2008;33:1671–9.
- Florides, G., Kalogirou, S.** (2007). Ground heat exchanger-A review of system model and applications, *Renewable Energy* 32 (2007) 2461–2478.
- Ingley, H. A., Wang, S. K., Rabl, A.** (2005). *Air Conditioning and Refrigeration, The CRC Handbook of Mechanical Engineering, 2th ed., CRC Press, Atlanta, USA*.
- Khalajzadeh, V., Heidarinejada, G., Srebrich, J.** (2011). Parameters optimization of a vertical ground heat exchanger based on response surface methodology, *Energy and Buildings* 43, 1288–1294.

- Koohi-Fayegh, S., Rosen, M.A.** (2014). An analytical approach to evaluating the effect of thermal interaction of geothermal heat exchangers on ground heat pump efficiency, *Energy Conversion and Management* 78 (2014) 184–192.
- Koohi-Fayegh, S., Rosen, M.A.** (2012). Examination of thermal interaction of multiple vertical ground heat exchangers, *Applied Energy*, 97 962–969.
- Kreith, F., Manglik, R., Bohn, M.** (2011). *Principles of Heat Transfer*, Seventh Edition, Stanford, USA.
- Lazzari, S., Priarone, A., Zanchini, E.** (2010). Long-term performance of BHE (borehole heat exchanger) fields with negligible groundwater movement, *Energy*, 35 4966-4974.
- Miyara, A., Tsubaki, K., Inoue, C., Yoshida, K.** (2011). Experimental study of several types of ground heat exchanger using a steel pilefoundation, *Renewable Energy* 36 (2011) 764-771.
- Ochsner, K.** (2007). *Geothermal heat pumps: a guide for planning and installing*. 1st ed.: Earthscan Publications Ltd.; London.
- Omer, A. M.** (2008). Ground-source heat pumps systems and applications. *Renewable Sustainable Energy* 2008;12:344–71.
- Ozgener O, Hepbasli A.** (2005). Experimental performance analysis of a solar assisted ground-source heat pump greenhouse heating system. *Energy Build* 2005;37:101–10.
- Ozisik, N.** (1993). *Heat conduction second edition.: A Wiley Inter science Publication* John Wiley & Sons, Inc, New Jersey USA.
- Park, S., Lee, D., Choi, H., Jung, K., Choi, M.** (2015). Relative constructability and thermal performance of cast-in-place concrete energy pile: Coil-type GHEX (ground heat exchanger) *Energy*, Volume 81, Pages 56-66.
- Rabin, Y., Korin, E.** (1996). Thermal analysis of a helical heat exchanger for ground thermal energy storage in arid zones, *International Journal of Heat and Mass Transfer* 39 (5) (1996) 1051e1065.
- Sagia, Z., Stegou, A., Rakopoulos, C.** (2012). Borehole resistance and heat conduction around vertical ground heat exchangers, *The Open Chemical Engineering Journal* 6 (2012) 32-40.
- Sauer, H. J., Howell, R. H.** (1983). *Heat Pump Systems*, John Wiley & Sons, NewYork,.
- Singh, A.** (2013). *Experimental study of Horizontal Ground Heat Exchanger* (MSc thesis)Department of mechanical engineering, Thapar University Patiala -147004, Indiana.
- Sivasakthivel, T., Murugesan, K., Thomas, H.R.** (2014). Optimization of operating parameters of ground source heat pump system for space heating and cooling by Taguchi method and utility concept, *Applied Energy* 116 76–85.

- Sporn, P., Ambrose, E. R., Baumeister, T.** (1947). Heat Pumps, John Wiley & Sons Inc. New York.
- Trillat-Berdal, V., Souyri, B., Fraisse, G.** (2006). Experimental study of a ground-coupled heat pump combined with thermal solar collectors. *Energy Build* 2006;38:1477–84.
- Wang, H., Qi, C., Du, H., Gu, J.** (2009). Thermal performance of borehole heat exchanger under groundwater flow, *Energy and Buildings* 41 (2009) 1368–1373.
- Wood, C.J., Liu, H., Riffat, S.B.** (2010). An investigation of the heat pump performance and ground temperature of a pile foundation heat exchanger system for a residential building. *Energy* 2010;35:4932–40.
- Zarrella, A., Carli, M.D., Galgaro, A.** (2013). Thermal performance of two types of energy foundation pile: helical pipe and triple U-tube. *Appl Therm Eng* 2013;61:301–10.
- Zarrella, A., Capozza, A., Carli, M.** (2013). Analysis of short helical and double U-tube borehole heat exchangers: a simulation-based comparison. *Appl Energy* 2013;112:358–70.
- Url-1** <http://energy.gov/energysaver/articles/geothermal-heat-pumps>, Date retrieved 20.04.2015
- Url-2** <https://www.geoexchange.org/>, Date retrieved 20.04.2015



APPENDIXES

APPENDIX A : ITU Energy Institute laboratory schematic view



CURRICULUM VITAE



Name Surname: Babak Dehghan
Place and Date of Birth: Iran, 14.12.1990
E-Mail: dehgan.babak@yahoo.com
B.Sc.: Mechanical Engineering, University of Tabriz, Iran
M.Sc.: Energy Science and Technology, Energy Institute, ITU

PROFESSIONAL EXPERIENCE AND REWARDS:

PUBLICATIONS, PRESENTATIONS AND PATENTS ON THE THESIS:

Babak Dehghan, Altug Sisman, Murat Aydin, "Optimum design of helix ground heat exchangers for heat pump applications", Energy and Building, *Submitted*, 2015

Babak Dehghan, Altug Sisman, Murat Aydin, "Optimizing the Distance between Boreholes with Helical Shaped Ground Heat Exchanger", World Geothermal Congress April 2015, Australia-New Zealand.

Murat Aydin, Altug Sisman, Ahmet Gultekin, **Babak Dehghan**, "Experimental and Computational Performance Comparison between Different Shallow Ground Heat Exchangers", World Geothermal Congress April 2015, Australia-New Zealand.

OTHER PUBLICATIONS, PRESENTATIONS AND PATENTS

Babak Dehghan, Rana Amirzehni, Burak Barutçu, " Short term wind speed prediction using artificial neural networks based on Levenberg-Marquardt Optimization Method", CIVILICA Encyclopedia of Civil Engineering, www.civilica.com

Babak Dehghan, Murat Aydin, Altug Sisman, "Long Term Performance Prediction of a Borehole Ground Heat Exchanger by Green's Function Method", World Geothermal Congress April 2015, Australia-New Zealand.

Babak Dehghan, Rana Amirzehni, Burak Barutçu, " Short term wind speed prediction using artificial neural networks Optimization Method", 13th International Conference on Clean Energy 2014, Istanbul-Turkey.

Babak Dehghan, Rana Amirzehni, Burak Barutçu,"Investigating the Applicability of Shallow Ground Heat Exchanger in Gas Turbine Inlet Air Cooling ", International Conference on Energy and Management, ICEM, June 2014, Istanbul Turkey.

